Advances in Nano Research, *Vol. 4, No. 3 (2016) 197-228*
DOI: http://dx.doi.org/10.12989/anr.2016.4.3.197

Thermal loading effects on electro-mechanical vibration behavior of piezoelectrically actuated inhomogeneous size-dependent Timoshenko nanobeams

Farzad Ebrahimi* and Erfan Salari

Department of Mechanical Engineering, Faculty of Engineering, Imam Khomeini International University, Qazvin, Iran

(Received May 22, 2016, Revised July 29, 2016, Accepted August 1, 2016)

Abstract. In the present study, thermo-electro-mechanical vibration characteristics of functionally graded piezoelectric (FGP) Timoshenko nanobeams subjected to in-plane thermal loads and applied electric voltage are carried out by presenting a Navier type solution for the first time. Three kinds of thermal loading, namely, uniform, linear and non-linear temperature rises through the thickness direction are considered. Thermo-electro-mechanical properties of FGP nanobeam are supposed to vary smoothly and continuously throughout the thickness based on power-law model. Eringen's nonlocal elasticity theory is exploited to describe the size dependency of nanobeam. Using Hamilton's principle, the nonlocal equations of motion together with corresponding boundary conditions based on Timoshenko beam theory are obtained for the free vibration analysis of graded piezoelectric nanobeams including size effect and they are solved applying analytical solution. According to the numerical results, it is revealed that the proposed modeling can provide accurate frequency results of the FGP nanobeams as compared to some cases in the literature. In following a parametric study is accompanied to examine the effects of several parameters such as various temperature distributions, external electric voltage, power-law index, nonlocal parameter and mode number on the natural frequencies of the size-dependent FGP nanobeams in detail. It is found that the small scale effect and thermo-electrical loading have a significant effect on natural frequencies of FGP nanobeams.

Keywords: functionally graded piezoelectric nanobeam; free vibration; Nonlocal elasticity theory; Thermal effect; Timoshenko beam theory

1. Introduction

Functionally graded materials (FGMs), a novel generation of composites of microscopical heterogeneity initiated by a group of Japanese scientists in the mid-1980s. In comparison with traditional composites, FGMs possess various advantages, for instance, ensuring smooth transition of stress distributions, minimization or elimination of stress concentration, and increased bonding strength along the interface of two dissimilar materials. In the last decade, beams and plates made of FGMs have found wide applications as structural elements in modern industries such as aeronautics/astronautics manufacturing industry, mechanical engineering and engine combustion

*Corresponding author, Assistant Professor, E-mail: febrahimy@eng.ikiu.ac.ir

http://www.techno-press.com/?journal=anr&subpage=7 ISSN: 2287-237X (Print), 2287-2388 (Online)

chamber, nuclear engineering and reactors. Motivated by these engineering applications, ceramic-metal FGMs have also attracted intensive research interests, which were mainly focused on their static, dynamic and vibration characteristics of FG structures (Ebrahimi *et al.* 2009).

The piezoelectric materials stand as a class of smart structures which are widely used as sensors and actuators in control systems due to their excellent electromechanical properties, easy fabrication, design flexibility, and efficiency to convert electrical energy into mechanical energy. The ability of piezoelectric materials to surpass the vibrational motion, shape control, and delay the buckling have necessitated more investigations on the behavior of structures including piezoelectricity effects (Ebrahimi and Rastgoo 2008). However, because of the superior properties of these smart materials, piezoelectric nanostructures have been regarded as the next-generation piezoelectric materials because of their inherent nanosized piezoelectricity. These distinct features make them suitable for potential applications in micro electro-mechanical systems (MEMS) and nano electro-mechanical systems (NEMS) such as nanogenerators (Wang and Song 2006), field effect transistors (Fei *et al.* 2009), piezoelectric gated diodes (He *et al.* 2007), gas sensors (Wan *et al.* 2004), nanowire resonators and oscillators (Tanner *et al.* 2007).

Moreover, nanoscale engineering materials have attracted great interest in modern science and technology after the invention of carbon nanotubes (CNTs) by Iijima (1991). They have significant mechanical, thermal and electrical performances that are superior to the conventional structural materials. Beam elements are one of the basic components in micro/nano electromechanical systems, biomedical sensors, actuators, transistors, probes, and resonators. In these nanodevices, the dimension may vary from several hundred nanometers to just a few nanometers. Therefore, understanding the mechanical and physical behaviors of the nanobeams made of piezoelectric materials or those incorporated with piezoelectric layer is of necessary in the design of the nanodevices.

The classical continuum theory is quite efficient in the mechanical analysis of the macroscopic structures, but its applicability to the identification of the size effect on the mechanical behaviors on micro- or nano-scale structures is questionable. This limitation of the classical continuum theory is partly due to the fact that the classical continuum theory does not admit the size dependence in the elastic solutions of inclusions and inhomogeneities. However the classical continuum models need to be extended to consider the nanoscale effects and this can be achieved through the nonlocal elasticity theory proposed by Eringen (2002) which consider the size-dependent effect. According to this theory, the stress state at a reference point is considered as a function of strain states of all points in the body. This nonlocal theory is proved to be in accordance with atomic model of lattice dynamics and with experimental observations on phonon dispersion (Eringen 1983). In the field of nonlocal elasticity theory, Pradhan and Mandal (2013) investigated the thermal vibration, buckling and bending characteristics of carbon nanotubes by using finite element method (FEM) based on Timoshenko beam theory. Ke *et al*. (2012a) and Ke and Wang (2012) studied the free vibration analysis of the piezoelectric Timoshenko nanobeams under thermo-electro-mechanical field based on the Eringen's theory. They noticed that the values of uniform temperature change, nonlocal parameter and applied voltage play a significant role in the vibrational response of the piezoelectric nanobeams.

Nowadays, with the development in nanotechnology, FGMs have also been employed in MEMS/NEMS (Witvrouw and Mehta 2005, Lee *et al.* 2006). Actually, FGMs find increasing applications in micro- and nano-scale structures such as thin films in the form of shape memory alloys (Fu *et al.* 2003, Lü *et al.* 2009), atomic force microscopes (AFMs) (Rahaeifard *et al.* 2009), micro sensors, micro piezoactuator and nano-motors (Carbonari *et al.* 2009, Lun *et al.* 2006). In all of these applications, the size effect plays major role which should be considered to study the mechanical behaviors of such small scale structures. Beams are the core structures widely used in MEMS, NEMS and AFMS with the order of microns or sub-microns, and their properties are closely related to their microstructures. On the other hands, FG nanobeams are important structural elements and hence, because of high sensitivity of MEMS/ NEMS to external stimulations, understanding mechanical properties and vibration behavior of them are of significant importance to the design and manufacture of FG MEMS/NEMS. Furthermore, different fabrication processes of nanoscale functionally graded material have been focused by the several researchers (Kim *et al.* 2009, Kerman *et al.* 2012). Therefore, establishing an accurate model of FG nanobeams is a key issue for successful NEMS design.

Based on the above discussions, thermal stability and free vibration characteristics of FG micro and nano structures have also been of interest of many investigators. Among them, Nateghi and Salamat-Talab (2013) investigated thermal effect on buckling and free vibration behavior of temperature-independent FG microbeams based on modified couple stress theory and using generalized differential quadrature (DQ) method. They showed that higher temperature changes signify size dependency of FG microbeam. Employing modified couple stress theory the nonlinear free vibration of FG microbeams based on von-Karman geometric nonlinearity was presented by Ke *et al*. (2012b). It is found that both the linear and nonlinear natural frequencies increase significantly when the thickness of the size-dependent FGM beam is comparable to the material length scale parameter. Eltaher *et al*. (2012) applied a finite element formulation for free vibration analysis of FG nanobeams based on nonlocal Euler beam theory. Also, Hosseini-Hashemi and Nazemnezhad (2013) in their study investigated nonlinear free vibration of simply supported Euler-Bernoulli FG nanobeams with considering surface effects and balance condition between the FG nanobeam bulk and its surfaces. In this study the multiple scales method was used as an analytical solution for the nonlinear governing equation. Additionally, using nonlocal simply supported Timoshenko beam theory, Rahmani and Pedram (2014) investigated vibration behavior of FG nanobeam by analytical method. Recently, Niknam and Aghdam (2015) have performed a semi analytical approach for large amplitude free vibration and buckling of FG nanobeams resting on elastic foundation based on nonlocal elasticity theory. They discussed that the effect of small scale parameter decreases by increasing length of the beam. More recently, Ebrahimi and Salari (2015a) analyzed the influences of various thermal environments on buckling and vibration of nonlocal temperature-dependent FG beams by using Navier analytical solution. In another work, Ebrahimi and Salari (2015b) investigated the thermo-mechanical vibration of FG nanobeams with arbitrary boundary conditions applying deferential transform method. Also, Ebrahimi *et al*. (2015a) explored the effects of linear and non-linear temperature distributions on vibration of FG nanobeams. Recently, Ebrahimi and Barati (2015a) presented a nonlocal higher-order shear deformation beam theory for vibration analysis of size-dependent functionally graded Nanobeams. They developed their previous works by analyzing thermal buckling and free vibration behavior of FG nanobeams based on the Timoshenko beam theory, too (Ebrahimi and Salari 2015b, c). It should be noted that the above mentioned studies dealt with the micro and nanobeams made of ceramic-metal functionally graded materials because of their high mechanical–thermal resistant. Also, Ebrahimi and Salari (2015d), Ebrahimi *et al*. (2015c) and examined the applicability of differential transformation method in investigations on vibrational characteristics of FG size-dependent nanobeams. In another work, Ebrahimi and Salari (2015e) presented a semi-analytical method for vibrational and buckling analysis of FG nanobeams considering the position of neutral axis.

Moreover, conventional piezoelectric sensors and actuators are often made of several layers of different piezoelectric materials. The principal weakness of these types of structures is that the high stress concentrations are usually appeared at the interlayer surfaces under mechanical or electrical loading. This drawback reduces the electrical field induced displacement characteristics, lifetime, integrity and reliability of piezoelectric devices, and also restricts the usefulness of piezoelectric actuators in the area of measured devices requiring high reliability. In order to overcome the aforementioned disadvantages of the traditional layered piezoelectric structures, a novel class of piezoelectric materials called functionally graded piezoelectric materials (FGPMs) has been presented and fabricated by using the metallurgical science and powder mold stacking press technique in which mechanical and electrical properties change continuously in one or more directions (Zhu and Meng 1995).

Finally, reported papers on FG piezoelectric materials subjected to thermo-electro-mechanical loads are limited in number. For instance, by using DQ method, the static bending, free vibration and dynamic analysis of monomorph, bimorph, and multimorph FGPM beams under the action of thermal, mechanical, and electrical loadings were presented by Yang and Xiang (2007) based on the Timoshenko beam theory. They assumed that the material properties of FGP beam graded in the thickness direction according to the power-law model. A closed form solution for the FGPM cantilever beams subjected to different loadings and based on the two dimensional theory of elasticity and the Airy stress function was proposed by Shi and Chen (2004). Additionally, based on the linear piezoelectricity theory, Zhong and Yu (2007) discussed a general solution on the electrostatic analysis of an FGP beam under various boundary conditions with arbitrary graded material properties along the beam thickness direction. Doroushi *et al*. (2011) used higher order shear deformation of Reddy beam theory to investigate thermo-electro-mechanical free and forced vibration analysis of FGPM beams. They solved their problem by using FE method. In another study, Komijani *et al*. (2013) analyzed nonlinear free vibration and post-buckling analysis of piezoelectric beams with graded properties based on Timoshenko beam theory. They showed that due to the non-symmetric distribution of material properties in the thickness direction, the linear critical buckling may not take place in this type of graded beams. Xiang and Shi (2009) predicted bending analysis of FGP sandwich cantilever under an applied electric field and heat conduction thermal load based on Airy stress function method. Also, thermo-mechanical geometrically non-linear static and dynamic analysis of FG beams integrated with a pair of sensor layers made of FGP materials were studied by Bodaghi *et al*. (2014). They concluded that the gradient indexes of FGP have a noticeable effect on their output voltages. Lezgy-Nazargah *et al*. (2013) recommended an efficient three nodded finite element model for static, free vibration and dynamic response of functionally graded piezoelectric material beams. The above reference has been recently extended to fully coupled thermo-mechanical analysis of bi-directional FG beams using a computationally low cost isogeometric finite element approach (Lezgy-Nazargah 2015). Also, Komijani *et al*. (2014) utilized modified couple stress theory to model the nonlinear deflection response of a monomorph microstructure-dependent FGPM beams based on Timoshenko beam theory. They also observed that the value of length scale parameter and the type of imposed load has significant effect on the nonlinear deflection behavior of FGPM beams.

To the authors' best knowledge, there is no work reported in the literature on the effects of various thermal environment and nanostructure dependency on the thermo-electro-mechanical vibration response of functionally graded piezoelectric nanobeams based on nonlocal elasticity theory. The common use of FGPM beams in high temperature environment leads to considerable changes in material properties. Consequently, thermal effects become important when the FGP

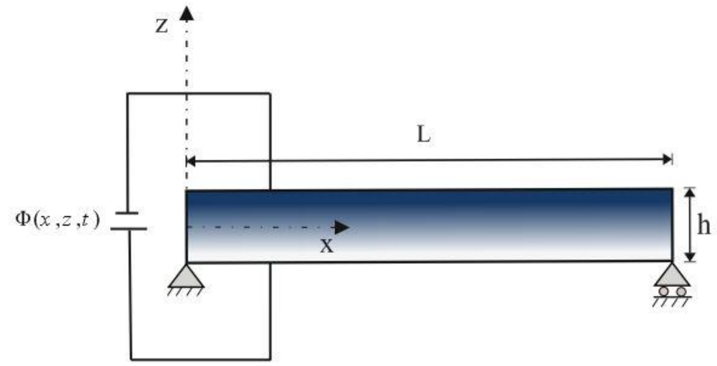

Fig. 1 Schematic configuration of a functionally graded piezoelectric nanobeam

nanodevices has to operate in either extremely hot or cold temperature environments. Therefore, there is strong scientific need to understand the vibration behavior of graded piezoelectric nanobeams under thermal and electrical loadings. According to this fact, in this study, vibration characteristics of FGP nanobeams considering the effect of three types of thermal loads namely, uniform, linear and non-linear temperature rises across the thickness is analyzed. An analytical method called Navier solution is employed for thermo-electrical vibration analysis of FG piezoelectric nanobeams for the first time. The thermo-electro-mechanical material properties of the beam is assumed to be graded in the thickness direction according to the power law distribution. Non- classical Timoshenko beam model and Eringen's nonlocal elasticity theory can capture size effect are employed. Governing equations and boundary conditions for the free vibration of a nonlocal FGP nanobeam have been derived via Hamilton's principle. These equations are solved using Navier type method and numerical solutions are obtained. The detailed mathematical derivations are presented while the emphasis is placed on investigating the effect of several parameters such as external electric voltage, different temperature distributions, power-law index, mode number and length scale parameter on vibration characteristics of size-dependent FGP nanobeams. Comparison between results of the present study and those available data in literature shows the accuracy of this model. Due to lack of similar results on the thermo-electrical response of FGP nanostructure, this study is likely to fill a gap in the state of the art of this problem.

2. Theoretical formulations

2.1 The material properties of FGP nanobeams

Consider a FGP nanobeam made of PZT-4 and PZT-5H piezoelectric materials with length L in x direction and uniform thickness h in z direction, and subjected to an electric potential $\Phi(x,z,t)$, as shown in Fig. 1. The effective material properties of the FGPM beam are assumed to vary continuously in the thickness direction (z-axis direction) according to a power function of the volume fractions of the constituents. Based on the power-law model, the effective material properties, P, can be considered as below (Komijani *et al.* 2014)

$$P = P_u V_u + P_l V_l \tag{1}$$

where (P_l, P_u) are the material properties at the lower and upper surfaces, respectively, and (V_l, V_u) are the corresponding volume fractions related by

$$V_u = (\frac{z}{h} + \frac{1}{2})^p, \quad V_l = 1 - V_u \tag{2}$$

Therefore, from Eqs. (1) and (2), the effective thermo-electro-mechanical material properties of the FGP beam can be expressed as

$$P(z) = \left(P_u - P_l\right)\left(\frac{z}{h} + \frac{1}{2}\right)^p + P_l \tag{3}$$

here p is the non-negative power-law exponent which determines the material distribution through the thickness of the beam and z is the distance from the mid-plane of the graded piezoelectric beam. According to this distribution, the top surface ($z=h/2$) of FGP nanobeam is PZT-4 rich, whereas the bottom surface ($z=-h/2$) is PZT-5H rich.

2.2 Nonlocal elasticity theory for the piezoelectric materials

Unlike the constitutive equation in classical elasticity, Eringen's nonlocal theory (Eringen 1983, 2002) states that the stress at a reference point x in a body is considered as a function of strains of all points x' in the near region. This assumption is agreement with experimental observations of atomic theory and lattice dynamics in phonon scattering in which for a homogeneous and nonlocal piezoelectric solid the basic equations with zero body force may be obtained as (Ke *et al*. 2012a)

$$\sigma_{ij} = \int_V \alpha\left(\left|x' - x\right|, \tau\right)\left[C_{ijkl}\varepsilon_{kl}(x') - e_{kij}E_k(x') - C_{ijkl}\alpha_{kl}\Delta T\right]dV(x') \tag{4a}$$

$$D_i = \int_V \alpha\left(\left|x' - x\right|, \tau\right)\left[e_{ikl}\varepsilon_{kl}(x') + k_{ik}E_k(x') + p_i\Delta T\right]dV(x') \tag{4b}$$

in which σ_{ij}, ε_{ij}, D_i and E_i are the stress, strain, electric displacement and electric field components, respectively; α_{kl} and ΔT are the thermal expansion coefficient and temperature change, respectively; C_{ijkl}, e_{kij}, k_{ik} and p_i are elastic, piezoelectric, dielectric and pyroelectric constants, respectively; $\alpha(|x'-x|,\tau)$ is the nonlocal kernel function and $|x'-x|$ is the Euclidean distance. $\tau=e_0a/l$ is defined as scale coefficient, where e_0 is a material constant which is determined experimentally or approximated by matching the dispersion curves of plane waves with those of atomic lattice dynamics; and a and l are the internal and external characteristic length of the nanostructures, respectively.

According to (Eringen 1983) it is possible to represent the integral constitutive relations given by Eq. (4) in an equivalent differential form as

$$\sigma_{ij} - (e_0 a)^2\nabla^2\sigma_{ij} = C_{ijkl}\varepsilon_{kl} - e_{kij}E_k - C_{ijkl}\alpha_{kl}\Delta T \tag{5a}$$

$$D_i - (e_0 a)^2\nabla^2 D_i = e_{ikl}\varepsilon_{kl} + k_{ik}E_k + p_i\Delta T \tag{5b}$$

where ∇^2 is the Laplacian operator; e_0a is called the nonlocal parameter revealing the size effect on the response of nanostructures.

2.3 Nonlocal FG piezoelectric nanobeam model

According to the Timoshenko beam theory, the displacements at any point of the beam, i.e., u_x and u_z along x and z directions, respectively, are assumed to be of the form

$$u_x\left(x,z,t\right)=u\left(x,t\right)+z\,\psi(x,t) \tag{6a}$$

$$u_z(x,z,t)=w(x,t) \tag{6b}$$

in which u and w are displacement components in the mid-plane along the coordinates x and z, respectively, while ψ denotes the total bending rotation of the cross-section and t is the time.

In order to satisfy Maxwell's equation in the quasi-static approximation, the distribution of electric potential along the thickness direction is assumed to vary as a combination of a cosine and linear variation which was proposed by (Wang 2002), as follows

$$\Phi(x,z,t)=-\cos(\beta z)\phi(x,t)+\frac{2z}{h}V_E \tag{7}$$

where $\beta=\pi/h$. Also, V_E is the initial external electric voltage applied to the FGP nanobeam; and $\phi(x,t)$ is the spatial function of the electric potential in the x-direction.

Considering strain-displacement relationships on the basis of Timoshenko beam theory, the non-zero strains can be written as:

$$\varepsilon_{xx}=\frac{\partial u}{\partial x}+z\,\frac{\partial \psi}{\partial x} \tag{8}$$

$$\gamma_{xz}=\frac{\partial w}{\partial x}+\psi \tag{9}$$

where ε_{xx} and γ_{xz} are the normal and shear components of strain tensor, respectively. Based on the assumed electric potential in Eq. (7), the non-zero components of electric field (E_x, E_z) can be obtained as

$$E_x=-\Phi_{,x}=\cos(\beta z)\frac{\partial \phi}{\partial x},\quad E_z=-\Phi_{,z}=-\beta\sin(\beta z)\phi-\frac{2V_E}{h} \tag{10}$$

In order to obtain the governing equations of motion, the Hamilton's principle can be stated in a dynamic form as

$$\int_0^t \delta(\Pi_S-\Pi_K+\Pi_W)\,dt=0 \tag{11}$$

here $\prod_S$ is strain energy, $\prod_K$ is kinetic energy and $\prod_W$ is work done by external applied forces. The first variation of strain energy $\prod_S$ can be calculated as

$$\delta\Pi_S=\int_0^L\int_{-h/2}^{h/2}\left(\sigma_{xx}\delta\varepsilon_{xx}+\sigma_{xz}\delta\gamma_{xz}-D_x\delta E_x-D_z\delta E_z\right)dzdx \tag{12}$$

Substituting Eqs. (8)-(10) into Eq. (12) yields

$$\begin{aligned}\delta\Pi_S &= \int_0^L \left(N_x \delta\left(\frac{\partial u}{\partial x}\right) + M_x \delta\left(\frac{\partial \psi}{\partial x}\right) + Q_x \delta\left(\psi + \frac{\partial w}{\partial x}\right)\right) dx \\ &+ \int_0^L \int_{-h/2}^{h/2} \left(-D_x \cos(\beta z)\,\delta\left(\frac{\partial \phi}{\partial x}\right) + D_z \beta \sin(\beta z)\,\delta\phi \right) dz dx\end{aligned} \tag{13}$$

in which N_x, M_x and Q_x are the axial force, bending moment and shear force resultants, respectively. Relations between the stress resultants and stress component used in Eq. (13) are defined as

$$N_x = \int_{-h/2}^{h/2} \sigma_{xx} dz\,, \quad M_x = \int_{-h/2}^{h/2} \sigma_{xx} z\, dz\,, \quad Q_x = \int_{-h/2}^{h/2} K_s\, \sigma_{xz}\, dz \tag{14}$$

here K_S=5/6 denotes the shear correction factor. In addition, the kinetic energy $\prod_K$ for graded piezoelectric nanobeam is formulated as

$$\Pi_K = \frac{1}{2}\int_0^L \int_{-h/2}^{h/2} \rho\left((\frac{\partial u_x}{\partial t})^2 + (\frac{\partial u_z}{\partial t})^2 \right) dz dx \tag{15}$$

where ρ is the mass density. From Eqs. (6) and (15), the first variation of the kinetic energy is presented as well by

$$\delta\Pi_K = \int_0^L \left[I_0 (\frac{\partial u}{\partial t}\frac{\partial \delta u}{\partial t} + \frac{\partial w}{\partial t}\frac{\partial \delta w}{\partial t}) + I_1 (\frac{\partial \psi}{\partial t}\frac{\partial \delta u}{\partial t} + \frac{\partial u}{\partial t}\frac{\partial \delta \psi}{\partial t}) + I_2 \frac{\partial \psi}{\partial t}\frac{\partial \delta \psi}{\partial t} \right] dx \tag{16}$$

where (I_0, I_1, I_2) are the mass moments of inertia, defined as follows

$$(I_0, I_1, I_2) = \int_{-h/2}^{h/2} \rho(1, z, z^2) dz \tag{17}$$

For a typical FGP nanobeam which has been in thermal environment for a long period of time, it is assumed that the temperature can be distributed across the thickness. Thus, three kinds of thermal loading such as uniform temperature rise, linear and nonlinear (heat conduction) temperature rises is taken into consideration. Hence, the work done due to initial thermal stresses (induced by the temperature rise) and external electric voltage, $\prod_W$, can be written in the form

$$\Pi_W = \frac{1}{2}\int_0^L \left[\left(N_T + N_E\right)\left(\frac{\partial w}{\partial x}\right)^2 \right] dx \tag{18}$$

where N_T and N_E are the normal forces induced by various temperature change ΔT and external electric voltage V_E, respectively, which can be expressed as

$$N_T = \int_{-h/2}^{h/2} c_{11}\alpha_1 (T - T_0) dz\,, \quad N_E = -\int_{-h/2}^{h/2} e_{31} \frac{2V_E}{h} dz \tag{19}$$

where T_0 is the reference temperature. For a FGPM nanobeam under thermo-electro-mechanical loading in the one dimensional case, the nonlocal constitutive relations (5a) and (5b) may be simplified as

$$\sigma_{xx} - (e_0 a)^2 \frac{\partial^2 \sigma_{xx}}{\partial x^2} = c_{11}\varepsilon_{xx} - e_{31}E_z - c_{11}\alpha_1 \Delta T \tag{20}$$

$$\sigma_{xz} - (e_0 a)^2 \frac{\partial^2 \sigma_{xz}}{\partial x^2} = c_{55}\gamma_{xz} - e_{15}E_x \tag{21}$$

$$D_x - (e_0 a)^2 \frac{\partial^2 D_x}{\partial x^2} = e_{15}\gamma_{xz} + k_{11}E_x \tag{22}$$

$$D_z - (e_0 a)^2 \frac{\partial^2 D_z}{\partial x^2} = e_{31}\varepsilon_{xx} + k_{33}E_z + p_3 \Delta T \tag{23}$$

Inserting Eqs. (13), (16) and (18) in Eq. (11) and integrating by parts, and collecting the coefficients of δu, δw, δ_ψ and δ_ϕ, the following governing equations are obtained

$$\frac{\partial N_x}{\partial x} = I_0 \frac{\partial^2 u}{\partial t^2} + I_1 \frac{\partial^2 \psi}{\partial t^2} \tag{24a}$$

$$\frac{\partial Q_x}{\partial x} - N_{x0} \frac{\partial^2 w}{\partial x^2} = I_0 \frac{\partial^2 w}{\partial t^2} \tag{24b}$$

$$\frac{\partial M_x}{\partial x} - Q_x = I_1 \frac{\partial^2 u}{\partial t^2} + I_2 \frac{\partial^2 \psi}{\partial t^2} \tag{24c}$$

$$\int_{-h/2}^{h/2} \left(\cos(\beta z) \frac{\partial D_x}{\partial x} + \beta \sin(\beta z) D_z \right) dz = 0 \tag{24d}$$

where $N_{x0}=N_T+N_E$. Furthermore, the corresponding natural and essential boundary conditions are defined at x=0 and x=L as follows

$$N = 0 \quad \text{or} \quad u = 0 \quad \text{at} \quad x = 0 \quad \text{and} \quad x = L \tag{25a}$$

$$Q = 0 \quad \text{or} \quad w = 0 \quad \text{at} \quad x = 0 \quad \text{and} \quad x = L \tag{25b}$$

$$M = 0 \quad \text{or} \quad \psi = 0 \quad \text{at} \quad x = 0 \quad \text{and} \quad x = L \tag{25c}$$

$$\int_{-h/2}^{h/2} D_x \cos(\beta z)\, dz = 0 \quad \text{or} \quad \phi = 0 \quad \text{at} \quad x = 0 \quad \text{and} \quad x = L \tag{25d}$$

By integrating Eqs. (20)-(23), the relations between local and nonlocal force-strain, moment-strain and other necessary nonlocal relations within the FGP Timoshenko nanobeam structure are achieved as

$$N_x - \mu \frac{\partial^2 N_x}{\partial x^2} = A_{xx} \frac{\partial u}{\partial x} + B_{xx} \frac{\partial \psi}{\partial x} + A_{31}^e \phi - N_T - N_E \tag{26}$$

$$M_x - \mu \frac{\partial^2 M_x}{\partial x^2} = B_{xx} \frac{\partial u}{\partial x} + D_{xx} \frac{\partial \psi}{\partial x} + E_{31} \phi \tag{27}$$

$$Q_x - \mu \frac{\partial^2 Q_x}{\partial x^2} = K_s C_{xz} (\frac{\partial w}{\partial x} + \psi) - K_s E_{15} \frac{\partial \phi}{\partial x} \tag{28}$$

$$\int_{-h/2}^{h/2} \left\{ D_x - \mu \frac{\partial^2 D_x}{\partial x^2} \right\} \cos(\beta z) dz = E_{15} (\frac{\partial w}{\partial x} + \psi) + F_{11} \frac{\partial \phi}{\partial x} \tag{29}$$

$$\int_{-h/2}^{h/2} \left\{ D_z - \mu \frac{\partial^2 D_z}{\partial x^2} \right\} \beta \sin(\beta z) dz = A_{31}^e \frac{\partial u}{\partial x} + E_{31} \frac{\partial \psi}{\partial x} - F_{33} \phi \tag{30}$$

where $\mu=(e_0 a)^2$ and other quantities are defined as

$$\{A_{xx}, B_{xx}, D_{xx}, C_{xz}\} = \int_{-h/2}^{h/2} \{c_{11}, z\, c_{11}, z^2 c_{11}, c_{55}\} dz \tag{31a}$$

$$\{A_{31}^e, E_{31}, E_{15}\} = \int_{-h/2}^{h/2} \{e_{31} \beta \sin(\beta z), z\, e_{31} \beta \sin(\beta z), e_{15} \cos(\beta z)\} dz \tag{31b}$$

$$\{F_{11}, F_{33}\} = \int_{-h/2}^{h/2} \{k_{11} \cos^2(\beta z), k_{33} \beta^2 \sin^2(\beta z)\} dz \tag{31c}$$

By substituting Eqs. (24a)-(24c), into Eqs. (26)-(28), the explicit relations of the nonlocal normal resultant force N_x, bending moment M_x and shear force Q_x can be derived as

$$N_x = A_{xx} \frac{\partial u}{\partial x} + B_{xx} \frac{\partial \psi}{\partial x} + A_{31}^e \phi - N_T - N_E + \mu (I_0 \frac{\partial^3 u}{\partial x \partial t^2} + I_1 \frac{\partial^3 \psi}{\partial x \partial t^2}) \tag{32}$$

$$M_x = B_{xx} \frac{\partial u}{\partial x} + D_{xx} \frac{\partial \psi}{\partial x} + E_{31} \phi + \mu (I_0 \frac{\partial^2 w}{\partial t^2} + I_1 \frac{\partial^3 u}{\partial x \partial t^2} + I_2 \frac{\partial^3 \psi}{\partial x \partial t^2} + N_{x0} \frac{\partial^2 w}{\partial x^2}) \tag{33}$$

$$Q_x = K_s C_{xz} (\frac{\partial w}{\partial x} + \psi) - K_s E_{15} \frac{\partial \phi}{\partial x} + \mu (I_0 \frac{\partial^3 w}{\partial x \partial t^2} + N_{x0} \frac{\partial^3 w}{\partial x^3}) \tag{34}$$

It should be pointed that substituting Eq. (24d) into Eqs. (29) and (30), does not lead to the explicit expressions for D_x and D_z as there are two unknowns and only one equilibrium Eq. (24d). However, by using Eqs. (29) and (30), Eq. (24d) can be re-expressed in terms of u, w, ψ and ϕ. Then, based on Timoshenko beam theory, the equations of motion for a nonlocal FG piezoelectric beam can be derived by substituting for N_x, M_x and Q_x from Eqs. (32)-(34) into Eqs. (24a)-(24c) as follows

$$A_{xx}\frac{\partial^2 u}{\partial x^2}+B_{xx}\frac{\partial^2 \psi}{\partial x^2}+A_{31}^e\frac{\partial \phi}{\partial x}+\mu\left(I_0\frac{\partial^4 u}{\partial t^2\partial x^2}+I_1\frac{\partial^4 \psi}{\partial t^2\partial x^2}\right)-I_0\frac{\partial^2 u}{\partial t^2}-I_1\frac{\partial^2 \psi}{\partial t^2}=0 \tag{35}$$

$$\begin{aligned}&K_sC_{xz}\left(\frac{\partial^2 w}{\partial x^2}+\frac{\partial \psi}{\partial x}\right)-K_sE_{15}\frac{\partial^2 \phi}{\partial x^2}-(N_T+N_E)\frac{\partial^2 w}{\partial x^2}-I_0\frac{\partial^2 w}{\partial t^2}\\&+\mu\left(I_0\frac{\partial^4 w}{\partial t^2\partial x^2}+(N_T+N_E)\frac{\partial^4 w}{\partial x^4}\right)=0\end{aligned} \tag{36}$$

$$\begin{aligned}&B_{xx}\frac{\partial^2 u}{\partial x^2}+D_{xx}\frac{\partial^2 \psi}{\partial x^2}+E_{31}\frac{\partial \phi}{\partial x}+\mu\left(I_1\frac{\partial^4 u}{\partial t^2\partial x^2}+I_2\frac{\partial^4 \psi}{\partial t^2\partial x^2}\right)-K_sC_{xz}\left(\frac{\partial w}{\partial x}+\psi\right)\\&+K_sE_{15}\frac{\partial \phi}{\partial x}-I_1\frac{\partial^2 u}{\partial t^2}-I_2\frac{\partial^2 \psi}{\partial t^2}=0\end{aligned} \tag{37}$$

$$E_{15}\left(\frac{\partial^2 w}{\partial x^2}+\frac{\partial \psi}{\partial x}\right)+F_{11}\frac{\partial^2 \phi}{\partial x^2}+A_{31}^e\frac{\partial u}{\partial x}+E_{31}\frac{\partial \psi}{\partial x}-F_{33}\phi=0 \tag{38}$$

3. Types of thermal distributions

3.1 Uniform temperature rise (UTR)

The FGP nanobeam initial temperature is assumed to be T_0=300K, which is a stress free state, uniformly changed to final temperature with ΔT. The temperature rise is given by

$$\Delta T=T-T_0 \tag{39}$$

3.2 Linear temperature rise (LTR)

Consider a graded nanobeam where the temperature of the upper surface (PZT-4-rich) is T_u and it is considered to vary linearly along the thickness from T_u to the lower surface (PZT-5H-rich) temperature T_l. Therefore, the temperature rise as a function of thickness is considered as below (Kiani and Eslami 2013)

$$T=T_l+\Delta T\left(\frac{1}{2}+\frac{z}{h}\right) \tag{40}$$

The ΔT in Eq. (40) could be defined $\Delta T=T_u-T_l$.

3.3 Nonlinear temperature rise (NLTR)

In such a case, nonlinear temperature rise across the thickness is assumed. The steady-state one-dimensional heat conduction equation with the known temperature boundary conditions on bottom and top surfaces of the FGP nanobeam can be obtained by solving the following equation (Zhang 2013)

$$-\frac{d}{dz}\left(\kappa(z)\frac{dT}{dz}\right)=0$$
$$T\left(\frac{h}{2}\right)=T_u\,,\quad T\left(-\frac{h}{2}\right)=T_l \tag{41}$$

where κ is the thermal conductivity coefficient. The solution of Eq. (41) subjected to the boundary conditions can be solved by the following equation

$$T=T_l+(\Delta T)\frac{\int_{-h/2}^{z}\frac{1}{\kappa(z)}dz}{\int_{-h/2}^{h/2}\frac{1}{\kappa(z)}dz} \tag{42}$$

where $\Delta T=T_u-T_l$.

4. Solution procedure

In this section, the analytical solutions of the governing equations for free vibration of FGPM nanobeam with simply supported (S-S) boundary conditions are derived by using Navier method. Also, it is assumed that the value of electric potential is equal to zero at the ends of the FGPM nanobeam. The displacement functions are expressed as product of undetermined coefficients and known trigonometric functions to satisfy the governing equations and the conditions at x=0, L. The following displacement fields are assumed to be of the form

$$u(x,t)=\sum_{n=1}^{\infty}U_n\cos\left(\frac{n\pi}{L}x\right)e^{i\omega_n t} \tag{43}$$

$$w(x,t)=\sum_{n=1}^{\infty}W_n\sin\left(\frac{n\pi}{L}x\right)e^{i\omega_n t} \tag{44}$$

$$\psi(x,t)=\sum_{n=1}^{\infty}\Psi_n\cos\left(\frac{n\pi}{L}x\right)e^{i\omega_n t} \tag{45}$$

$$\phi(x,t)=\sum_{n=1}^{\infty}\Phi_n\sin\left(\frac{n\pi}{L}x\right)e^{i\omega_n t} \tag{46}$$

where U_n, W_n, Ψ_n and Φ_n are the unknown Fourier coefficients to be determined for each n value. The boundary conditions for simply supported FGP beam can be identified as

$$u(0)=0,\quad \frac{\partial u}{\partial x}(L)=0,\quad w(0)=w(L)=0 \tag{47}$$

$$\frac{\partial \psi}{\partial x}(0) = \frac{\partial \psi}{\partial x}(L) = 0, \quad \phi(0) = \phi(L) = 0$$

Substituting Eqs. (43)-(46) into Eqs. (35)-(38) respectively, leads to Eqs. (48)-(51)

$$\left(-A_{xx} (\frac{n\pi}{L})^2 + I_0 (1 + \mu (\frac{n\pi}{L})^2) \omega_n{}^2 \right) U_n + \left(-B_{xx} (\frac{n\pi}{L})^2 + I_1 (1 + \mu (\frac{n\pi}{L})^2) \omega_n{}^2 \right) \Psi_n + \left(A_{31}^e (\frac{n\pi}{L}) \right) \Phi_n = 0 \tag{48}$$

$$\left(-K_s C_{xz} (\frac{n\pi}{L})^2 + (N_T + N_E) (\frac{n\pi}{L})^2 (1 + \mu (\frac{n\pi}{L})^2) + I_0 (1 + \mu (\frac{n\pi}{L})^2) \omega_n{}^2 \right) W_n - \left(K_s C_{xz} (\frac{n\pi}{L}) \right) \Psi_n + \left(K_s E_{15} (\frac{n\pi}{L})^2 \right) \Phi_n = 0 \tag{49}$$

$$\left(-B_{xx} (\frac{n\pi}{L})^2 + I_1 (1 + \mu (\frac{n\pi}{L})^2) \omega_n{}^2 \right) U_n - \left(K_s C_{xz} (\frac{n\pi}{L}) \right) W_n + \left(-D_{xx} (\frac{n\pi}{L})^2 - K_s C_{xz} + I_2 (1 + \mu (\frac{n\pi}{L})^2) \omega_n{}^2) \right) \Psi_n + \left(E_{31} (\frac{n\pi}{L}) + K_s E_{15} (\frac{n\pi}{L}) \right) \Phi_n = 0 \tag{50}$$

$$\left(-A_{31}^e (\frac{n\pi}{L}) \right) U_n - \left(E_{15} (\frac{n\pi}{L})^2 \right) W_n - \left(E_{15} (\frac{n\pi}{L}) + E_{31} (\frac{n\pi}{L}) \right) \Psi_n - \left(F_{11} (\frac{n\pi}{L})^2 + F_{33} \right) \Phi_n = 0 \tag{51}$$

By setting the determinant of the coefficient matrix of the above equations, the nontrivial analytical solutions can be obtained from the following equations

$$\left\{ ([K] + \Delta T\,[K_T]) - \bar{\omega}^2 [M] \right\} \begin{Bmatrix} U_n \\ W_n \\ \Psi_n \\ \Phi_n \end{Bmatrix} = 0 \tag{52}$$

where [K] and [K_T] are stiffness matrix and the coefficient matrix of temperature change, respectively, and [M] is the mass matrix. By setting this polynomial to zero, we can find natural frequencies $\bar{\omega}_n$ of the FGP nanobeam subjected to thermo-electrical loading.

5. Results and discussion

In this section, the thermo-electro-mechanical free vibration of an FGPM nanobeam in thermal environments is investigated through some numerical examples and some comparisons are made between the results obtained from Navier solution method and other numerical technique so that the accuracy of present work is verified. Also, to demonstrate the applied electric voltage and

Table 1 Thermo-electro-mechanical coefficients of material properties for PZT-4 and PZT-5H (Doroushi *et al.* 2011)

Properties	PZT-4	PZT-5H
c_{11} (GPa)	81.3	60.6
c_{55} (GPa)	25.6	23.0
e_{31} (Cm^{-2})	-10.0	-16.604
e_{15} (Cm^{-2})	40.3248	44.9046
k_{11} (C^{2}m^{-2}N^{-1})	0.6712e-8	1.5027e-8
k_{33} (C^{2}m^{-2}N^{-1})	1.0275e-8	2.554e-8
α_1 (K^{-1})	2.0e-6	10.0e-6
κ (Wm^{-1}K^{-1})	2.1	1.5
p_3 (Cm^{-2} K^{-1})	2.5e-5	0.548e-5
ρ (kgm^{-3})	7500	7500

nonlocal parameter effects on the thermo-mechanical vibration analysis of FGP nanobeams, variations of the natural frequencies versus temperature rise, external electric voltage, power law index, and thickness ratios of the FG piezoelectric nanobeam, are presented in this section. To this end, the nonlocal FGP beam made of PZT-4 and PZT-5H, with thermo-electro-mechanical material properties listed in Table 1, is considered. The bottom surface of the graded nanobeam is PZT-5H rich, whereas the top surface of the beam is PZT-4 rich. The beam geometry has the following dimensions: L (length)=10 nm and h (thickness)=varied. Also, it is assumed that the temperature increase in lower surface to reference temperature T_0 of the FGP nanobeam is T_l–T_0=5K (Kiani and Eslami 2013). Relation described in Eq. (53) are performed in order to calculate the non-dimensional natural frequencies

$$\bar{\omega} = \omega L^2 \sqrt{(\rho A / c_{11} I)_{\text{PZT-4}}} \tag{53}$$

where I=h^3/12 is the moment of inertia of the cross section of the beam. The numerical or analytical results for the thermoelectrically vibration of FGP nanobeam based on the nonlocal elasticity theory are not available in the literature. When no piezoelectric effect being taken into account, Eqs. (35)-(38) reduce to the model for FG nanobeam based on nonlocal elasticity theory. As part of the validation of the present method, a comparison study is performed to check the reliability of the present method and formulation. For this purpose, the FG nanobeams consist of Steel and Alumina with the material properties E_m=70 GPa, v_m= 0.3, ρ_m=7800 kgm^{-3} for Steel and E_m=390 GPa, v_m=0.24, ρ_m=3960 kgm^{-3} for Alumina. Thus to check the accuracy of the developed model, in Table 2, the fundamental frequency of S-S FG nanobeams are compared with those of Rahmani and Pedram (2014) which has been obtained by analytical solution for various values of the gradient index and nonlocality parameter. It is obvious from Table 2 that there is good agreement between the two results. After extensive validation of the present formulation, the effects of different parameters such as electric voltage, various temperature rise, nonlocality and gradient index on free vibration behavior of FGP nanobeam are investigated. The effect of the external electric voltage (V_E), gradient index (p) and nonlocal parameter (μ) on the vibration behavior of the S-S graded piezoelectric nanobeam for L/h=20 and based on analytical Navier solution method is examined and scrutinized in Tables 3-5 that list the variation of the first three

Table 2 Comparison of the non-dimensional fundamental frequency for a S-S FG nanobeam with various volume fraction index (L/h=20)

μ (nm)^2	p=0		p=0.5		p=1		p=5	
	Rahmani and Pedram(2014)	Present	Rahmani and Pedram(2014)	Present	Rahmani and Pedram(2014)	Present	Rahmani and Pedram(2014)	Present
0	9.8296	9.829567	7.7149	7.714917	6.9676	6.967612	5.9172	5.197206
1	9.3777	9.377684	7.3602	7.360249	6.6473	6.647298	5.6452	5.645181
2	8.9829	8.982892	7.0504	7.050389	6.3674	6.367453	5.4075	5.407524
3	8.6341	8.634101	6.7766	6.776634	6.1202	6.120215	5.1975	5.197559
4	8.3230	8.323019	6.5325	6.532475	5.8997	5.899707	5.0103	5.010294

Table 3 Effect of external electric voltage and temperature change on non-dimensional frequency of a S-S FGP nanobeam subjected to uniform temperature rise (L/h=20)

μ (nm)^2	V_E (V)	$\bar{\omega}_i$	ΔT=20 [K]			ΔT=50 [K]			ΔT=80 [K]		
			Gradient index			Gradient index			Gradient index		
			0.5	1	2	0.5	1	2	0.5	1	2
0	- 0.5	1	10.4514	10.3184	10.2265	10.1654	9.9641	9.8082	9.8711	9.5967	9.3713
		2	39.9879	39.3784	38.9264	39.6936	39.0139	38.4961	39.3971	38.6460	38.0609
		3	88.2271	86.8368	85.7950	87.9302	86.4692	85.3609	87.6324	86.0999	84.9246
	0	1	9.7489	9.5393	9.3717	9.4416	9.1549	8.9135	9.1240	8.7537	8.4304
		2	39.2759	38.5894	38.0612	38.9763	38.2173	37.6210	38.6743	37.8416	37.1755
		3	87.5110	86.0433	84.9250	87.2118	85.6722	84.4864	86.9115	85.2996	84.0456
	+ 0.5	1	8.9916	8.6907	8.4308	8.6575	8.2669	7.9183	8.3100	7.8202	7.3703
		2	38.5508	37.7837	37.1758	38.2455	37.4038	36.7250	37.9377	37.0198	36.2685
		3	86.7891	85.2424	84.0459	86.4873	84.8678	83.6028	86.1845	84.4916	83.1573
2	- 0.5	1	9.6393	9.5225	9.4435	9.3284	9.1374	8.9890	9.0068	8.7354	8.5101
		2	30.1915	29.7530	29.4332	29.8007	29.2688	28.8616	29.4046	28.7765	28.2785
		3	53.4950	52.6920	52.1001	53.0040	52.0838	51.3821	52.5085	51.4685	50.6540
	0	1	8.8727	8.6722	8.5105	8.5339	8.2475	8.0032	8.1812	7.7997	7.4614
		2	29.2420	28.7005	28.2790	28.8383	28.1983	27.6836	28.4288	27.6869	27.0751
		3	52.3056	51.3737	50.6546	51.8034	50.7498	49.9159	51.2962	50.1181	49.1660
	+ 0.5	1	8.0333	7.7289	7.4618	7.6575	7.2492	6.8775	7.2623	6.7354	6.2387
		2	28.2607	27.6079	27.0756	27.8427	27.0854	26.4531	27.4184	26.5527	25.8157
		3	51.0886	50.0208	49.1666	50.5743	49.3798	48.4052	50.0546	48.7303	47.6316
4	- 0.5	1	9.0121	8.9082	8.8396	8.6788	8.4953	8.3523	8.3321	8.0613	7.8346
		2	25.3962	25.0447	24.7930	24.9303	24.4675	24.1117	24.4554	23.8765	23.4106
		3	42.1974	41.5941	41.1573	41.5732	40.8210	40.2446	40.9395	40.0329	39.3108
	0	1	8.1870	7.9929	7.8351	7.8186	7.5299	7.2808	7.4319	7.0366	6.6806
		2	24.2597	23.7848	23.4111	23.7715	23.1763	22.6884	23.2731	22.5514	21.9418
		3	40.6790	39.9110	39.3115	40.0312	39.1046	38.3549	39.3727	38.2812	37.3738
	+ 0.5	1	7.2689	6.9581	6.6811	6.8513	6.4210	6.0215	6.4065	5.8347	5.2802
		2	23.0674	22.4543	21.9424	22.5534	21.8087	21.1696	22.0274	21.1434	20.3674
		3	39.1017	38.1537	37.3746	38.4273	37.3094	36.3671	37.7408	36.4454	35.3309

Table 4 Effect of external electric voltage and temperature change on non-dimensional frequency of a S-S FGP nanobeam subjected to linear temperature rise (L/h=20)

μ (nm)^2	V_E (V)	$\bar{\omega}_i$	ΔT=20 [K]			ΔT=50 [K]			ΔT=80 [K]		
			Gradient index			Gradient index			Gradient index		
			0.5	1	2	0.5	1	2	0.5	1	2
0	- 0.5	1	10.5162	10.3970	10.3138	10.4022	10.2542	10.1381	10.2870	10.1094	9.9593
		2	40.0554	39.4605	39.0180	39.9368	39.3117	38.8344	39.8179	39.1623	38.6500
		3	88.2953	86.9199	85.8877	88.1755	86.7694	85.7020	88.0555	86.6186	85.5159
	0	1	9.8183	9.6242	9.4669	9.6961	9.4698	9.2752	9.5724	9.3128	9.0795
		2	39.3446	38.6731	38.1548	39.2240	38.5212	37.9671	39.1029	38.3688	37.7785
		3	87.5798	86.1271	85.0186	87.4590	85.9752	84.8310	87.3381	85.8230	84.6430
	+ 0.5	1	9.0669	8.7838	8.5365	8.9344	8.6143	8.3234	8.8000	8.4415	8.1047
		2	38.6208	37.8694	37.2717	38.4979	37.7143	37.0795	38.3745	37.5585	36.8864
		3	86.8585	85.3270	84.1405	86.7367	85.1737	83.9510	86.6147	85.0201	83.7610
2	- 0.5	1	9.7095	9.6076	9.5380	9.5859	9.4529	9.3478	9.4607	9.2956	9.1536
		2	30.2809	29.8615	29.5541	30.1239	29.6645	29.3114	29.9661	29.4663	29.0666
		3	53.6075	52.8287	52.2525	53.4099	52.5807	51.9468	53.2116	52.3315	51.6392
	0	1	8.9489	8.7655	8.6153	8.8147	8.5957	8.4042	8.6784	8.4225	8.1876
		2	29.3343	28.8130	28.4048	29.1722	28.6088	28.1522	29.0092	28.4032	27.8973
		3	52.4207	51.5140	50.8114	52.2186	51.2596	50.4969	52.0158	51.0040	50.1805
	+ 0.5	1	8.1174	7.8335	7.5811	7.9692	7.6430	7.3403	7.8182	7.4476	7.0913
		2	28.3561	27.7248	27.2070	28.1884	27.5126	26.9432	28.0197	27.2987	26.6767
		3	51.2064	50.1648	49.3281	50.9995	49.9036	49.0042	50.7918	49.6409	48.6780
4	- 0.5	1	9.0871	8.9991	8.9405	8.9550	8.8338	8.7373	8.8208	8.6653	8.5292
		2	25.5023	25.1736	24.9365	25.3157	24.9396	24.6483	25.1278	24.7034	24.3568
		3	42.3399	41.7672	41.3501	42.0895	41.4531	40.9631	41.8375	41.1366	40.5724
	0	1	8.2696	8.0940	7.9487	8.1241	7.9098	7.7194	7.9760	7.7212	7.4831
		2	24.3708	23.9204	23.5630	24.1755	23.6741	23.2579	23.9786	23.4252	22.9487
		3	40.8268	40.0914	39.5133	40.5671	39.7640	39.1081	40.3056	39.4339	38.6987
	+ 0.5	1	7.3617	7.0741	6.8141	7.1980	6.8625	6.5451	7.0304	6.6442	6.2647
		2	23.1842	22.5979	22.1044	22.9788	22.3370	21.7788	22.7715	22.0730	21.4483
		3	39.2555	38.3424	37.5869	38.9853	37.9999	37.1606	38.7131	37.6544	36.7295

dimensionless frequencies of FGP beam subjected to uniform (UTR), linear (LTR) and nonlinear temperature rises (NLTR), respectively. It is evident from the results of the tables that increasing the nonlocality parameter yields the reduction in dimensionless frequencies for every material graduation and temperature change, which these observations mean that the small scale effects in the nonlocal model make FGP nanobeams more flexible. It can also be deduced from these tables that the first three non-dimensional frequencies decrease by increasing temperature change (UTR, LTR and NLTR) and it can be emphasized that temperature change has a significant effect on the dimensionless natural frequencies, especially for lower mode numbers. It can be stated that the natural frequencies predicted by UTR loading are always smaller than those evaluated by LTR and NLTR and this situation is more prominent for smaller nonlocality parameter. In addition, it is

Table 5 Effect of external electric voltage and temperature change on non-dimensional frequency of a S-S FGP nanobeam subjected to non-linear temperature rise (L/h=20)

μ (nm)^2	V_E (V)	$\bar{\omega}_i$	ΔT=20 [K]			ΔT=50 [K]			ΔT=80 [K]		
			Gradient index			Gradient index			Gradient index		
			0.5	1	2	0.5	1	2	0.5	1	2
0	- 0.5	1	10.5120	10.3904	10.3060	10.3917	10.2374	10.1182	10.2699	10.0822	9.9268
		2	40.0510	39.4536	39.0097	39.9259	39.2943	38.8138	39.8005	39.1343	38.6168
		3	88.2909	86.9129	85.8793	88.1645	86.7518	85.6811	88.0379	86.5904	85.4824
	0	1	9.8138	9.6171	9.4584	9.6848	9.4517	9.2534	9.5541	9.2833	9.0438
		2	39.3402	38.6661	38.1464	39.2129	38.5035	37.9460	39.0851	38.3403	37.7445
		3	87.5754	86.1200	85.0102	87.4480	85.9575	84.8099	87.3203	85.7946	84.6092
	+ 0.5	1	9.0621	8.7760	8.5271	8.9222	8.5944	8.2991	8.7801	8.4088	8.0648
		2	38.6163	37.8622	37.2631	38.4866	37.6961	37.0579	38.3564	37.5294	36.8515
		3	86.8540	85.3199	84.1320	86.7255	85.1558	83.9297	86.5968	84.9914	83.7268
2	- 0.5	1	9.7050	9.6004	9.5296	9.5745	9.4347	9.3262	9.4422	9.2660	9.1182
		2	30.2751	29.8524	29.5432	30.1095	29.6415	29.2840	29.9429	29.4291	29.0224
		3	53.6003	52.8172	52.2388	53.3918	52.5517	51.9123	53.1825	52.2849	51.5837
	0	1	8.9440	8.7577	8.6059	8.8023	8.5757	8.3801	8.6582	8.3898	8.1481
		2	29.3284	28.8035	28.3935	29.1573	28.5849	28.1237	28.9852	28.3646	27.8512
		3	52.4133	51.5022	50.7973	52.2001	51.2299	50.4614	51.9859	50.9562	50.1234
	+ 0.5	1	8.1120	7.8247	7.5704	7.9555	7.6205	7.3127	7.7958	7.4106	7.0456
		2	28.3500	27.7150	27.1952	28.1730	27.4877	26.9134	27.9949	27.2586	26.6258
		3	51.1988	50.1527	49.3136	50.9805	49.8730	48.9676	50.7612	49.5918	48.6191
4	- 0.5	1	9.0823	8.9915	8.9315	8.9428	8.8143	8.7142	8.8010	8.6335	8.4913
		2	25.4955	25.1627	24.9236	25.2986	24.9122	24.6157	25.1001	24.6591	24.3040
		3	42.3307	41.7526	41.3328	42.0664	41.4163	40.9194	41.8004	41.0772	40.5017
	0	1	8.2643	8.0855	7.9386	8.1106	7.8880	7.6932	7.9540	7.6855	7.4398
		2	24.3637	23.9090	23.5494	24.1575	23.6452	23.2233	23.9496	23.3784	22.8926
		3	40.8173	40.0762	39.4952	40.5432	39.7257	39.0623	40.2671	39.3720	38.6246
	+ 0.5	1	7.3558	7.0644	6.8022	7.1828	6.8374	6.5142	7.0054	6.6027	6.2129
		2	23.1767	22.5858	22.0899	22.9598	22.3064	21.7419	22.7409	22.0234	21.3883
		3	39.2456	38.3265	37.5678	38.9604	37.9598	37.1124	38.6730	37.5896	36.6514

indicated that increase the power indexes lead to a decrease of the dimensionless frequency. This is because that as increasing the value of gradient index the percentage of PZT-5H phase will rise, thus making such FGP nanobeams more flexible. At the same time, there is no available data for the natural frequency of FGP nanobeams as far as the author knows. Therefore, it is believed that the tabulated results can be useful reference for future studies. The fundamental frequency parameter versus temperature rise is presented in Figs. 2-4 for the UTR, LTR and NLTR cases of thermal loading, respectively. In these figures, the non-dimensional frequency of simply supported FGPM nanobeam is plotted as a function of the external electric voltage for the selected values of the nonlocal parameter (μ=0,1,2,3,4) and gradient index p=0.5 at constant slenderness ratio

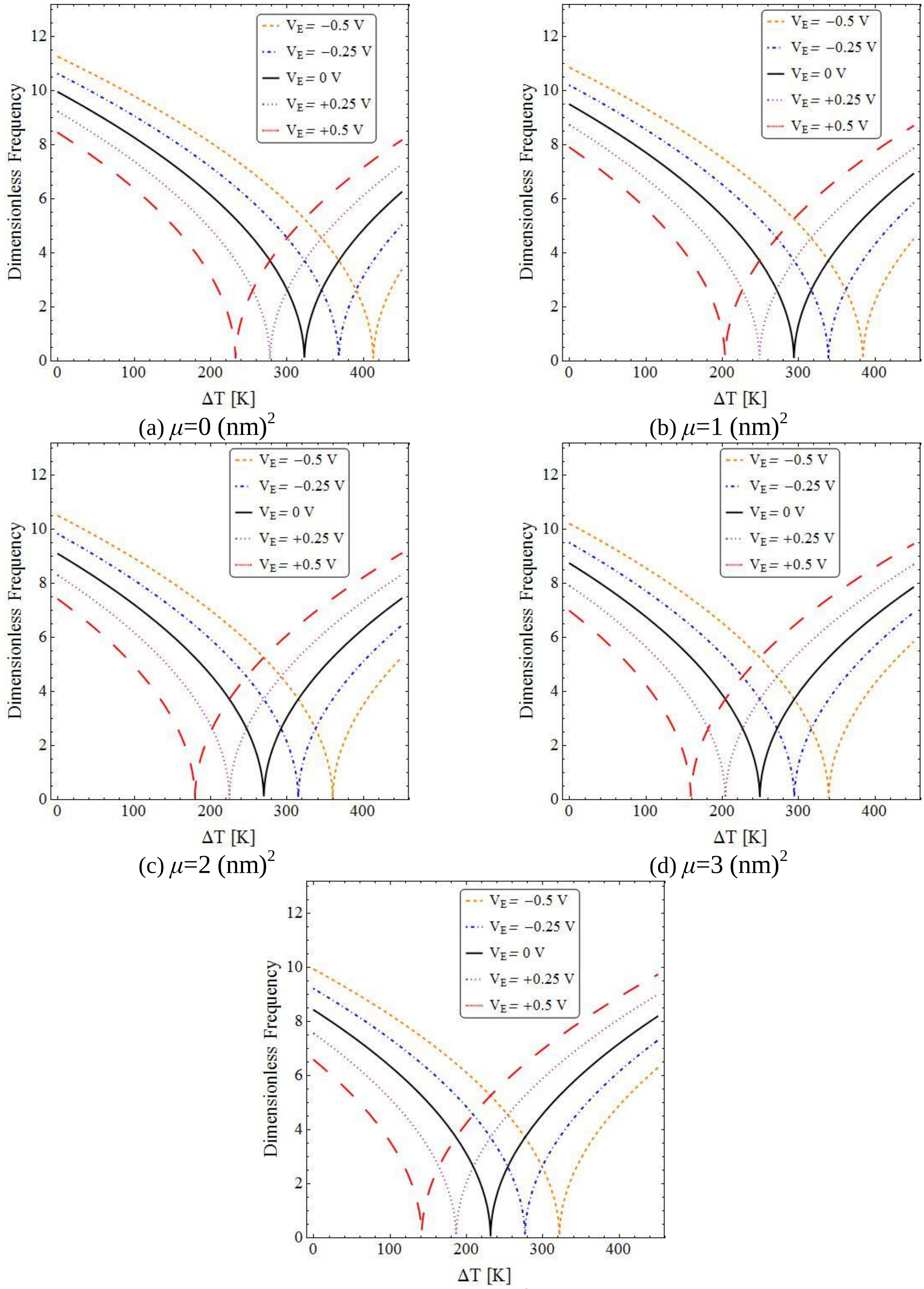

(a) μ=0 (nm)^2 (b) μ=1 (nm)^2

(c) μ=2 (nm)^2 (d) μ=3 (nm)^2

(e) μ=4 (nm)^2

Fig. 2 Effect of external electric voltage on the dimensionless frequency of the S-S FGP nanobeam with respect to uniform temperature rise for different values of nonlocal parameters (p=0.5, L/h=25)

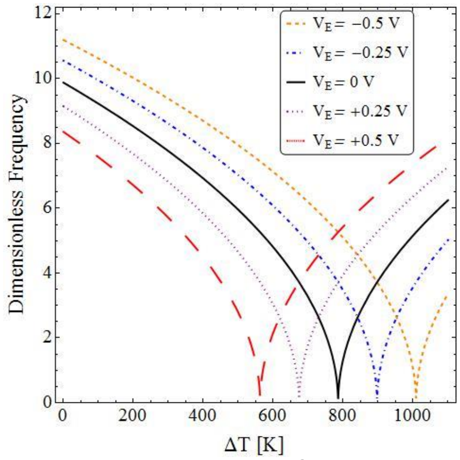

(a) μ=0 (nm)^2

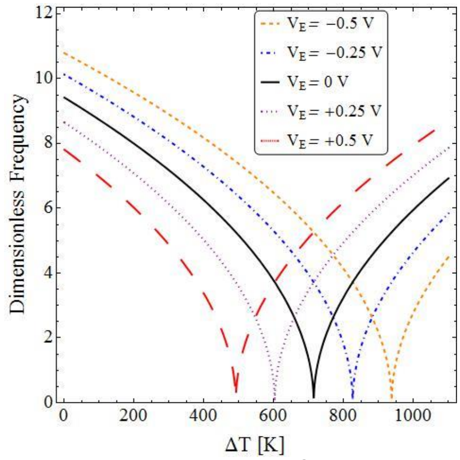

(b) μ=1 (nm)^2

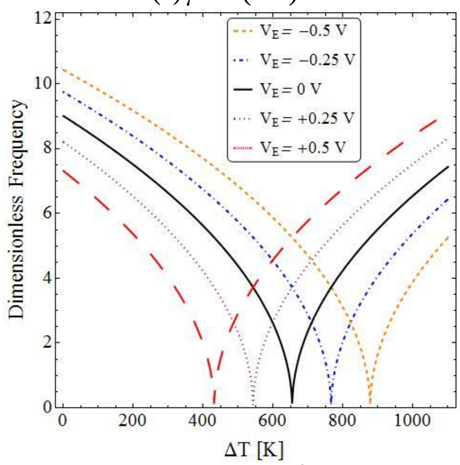

(c) μ=2 (nm)^2

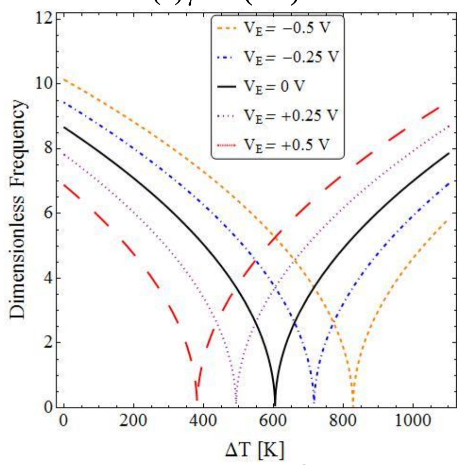

(d) μ=3 (nm)^2

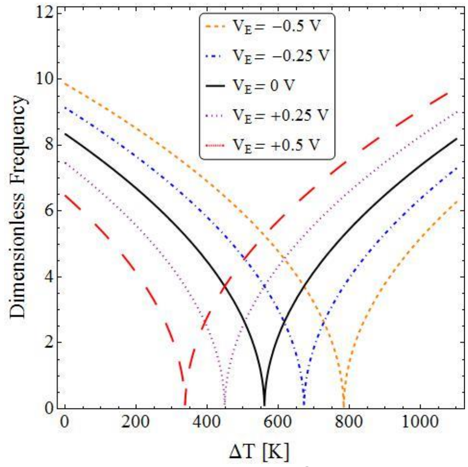

(e) μ=4 (nm)^2

Fig. 3 Effect of external electric voltage on the dimensionless frequency of the S-S FGP nanobeam with respect to linear temperature rise for different values of nonlocal parameters (p=0.5, L/h=25)

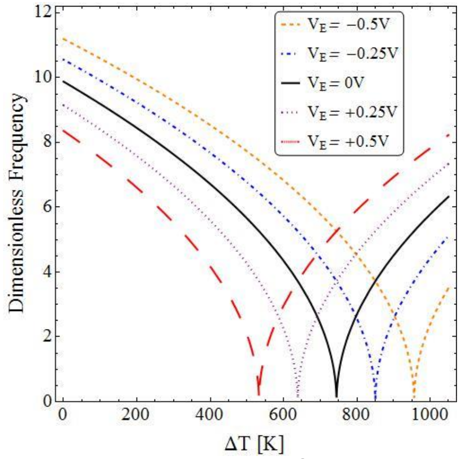

(a) μ=0 (nm)^2

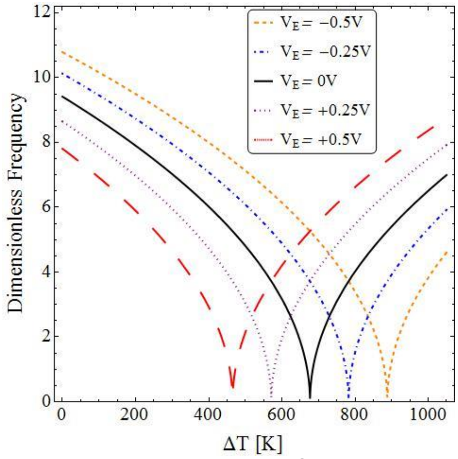

(b) μ=1 (nm)^2

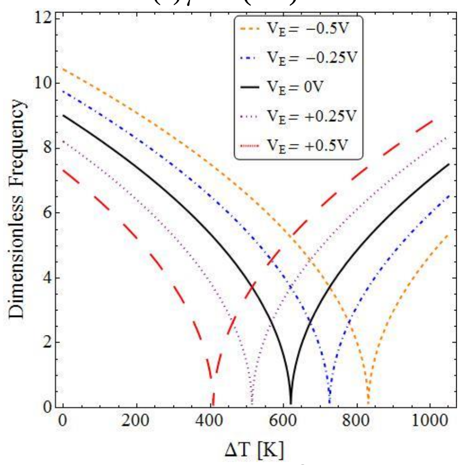

(c) μ=2 (nm)^2

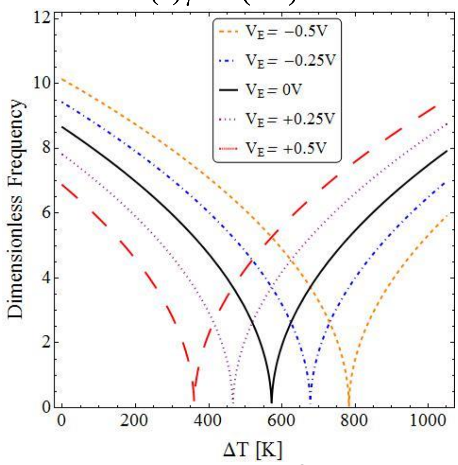

(d) μ=3 (nm)^2

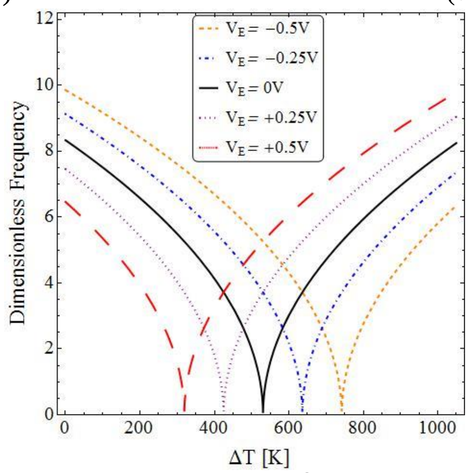

(e) μ=4 (nm)^2

Fig. 4 Effect of external electric voltage on the dimensionless frequency of the S-S FGP nanobeam with respect to non-linear temperature rise for different values of nonlocal parameters (p=0.5, L/h=25)

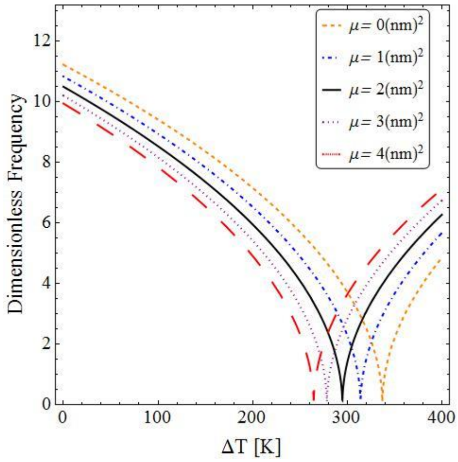

(a) V_E=−0.5 V

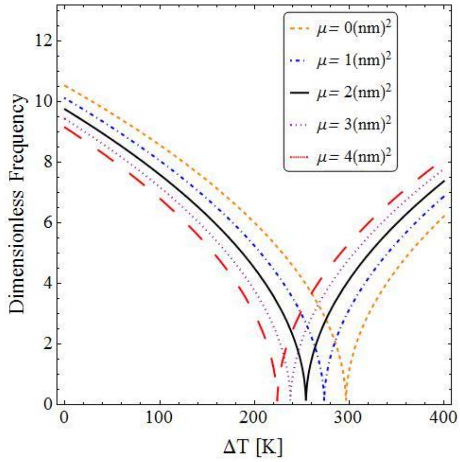

(a) V_E=−0.25 V

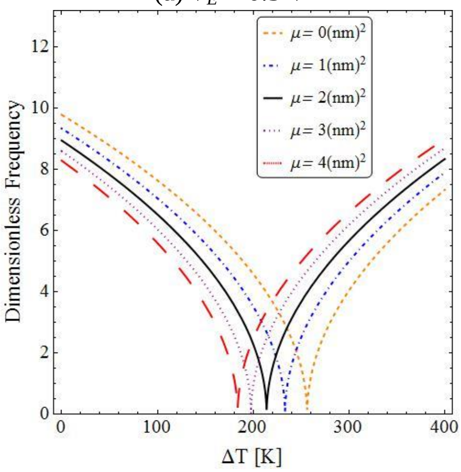

(c) V_E=0 V

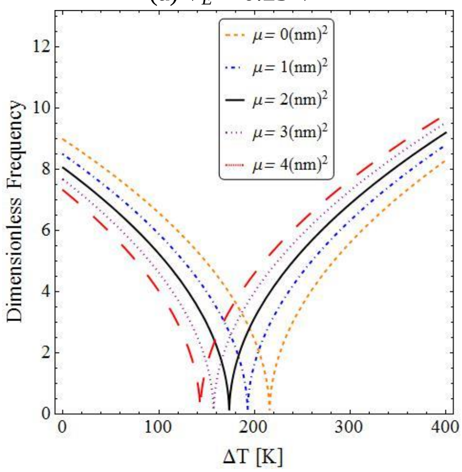

(d) V_E=0.25 V

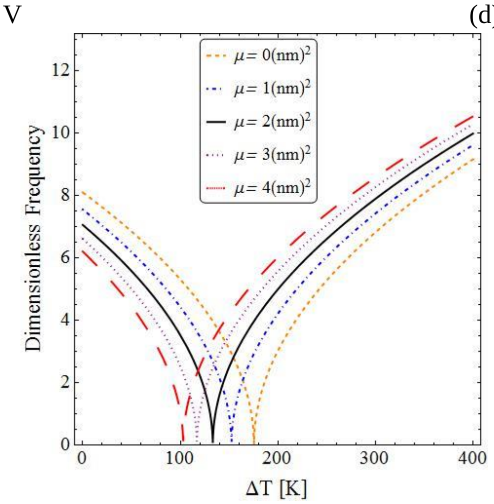

(e) V_E=0.5 V

Fig. 5 Effect of nonlocal parameter on the dimensionless frequency of the S-S FGP nanobeam with respect to uniform temperature rise for different values of external electric voltage (p=1, L/h=25)

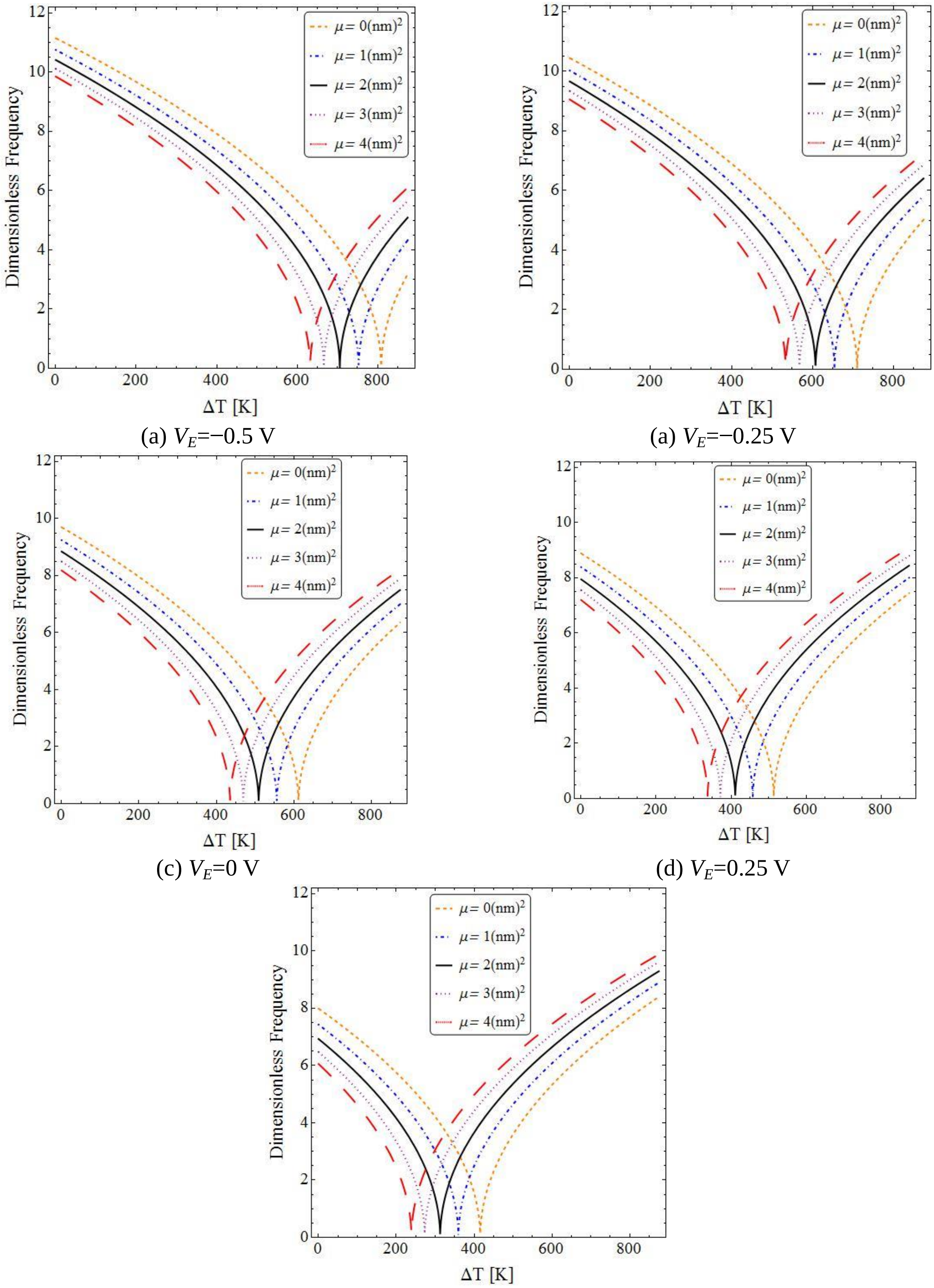

(a) V_E=−0.5 V

(a) V_E=−0.25 V

(c) V_E=0 V

(d) V_E=0.25 V

(e) V_E=0.5 V

Fig. 6 Effect of nonlocal parameter on the dimensionless frequency of the S-S FGP nanobeam with respect to linear temperature rise for different values of external electric voltage (p=1, L/h=25)

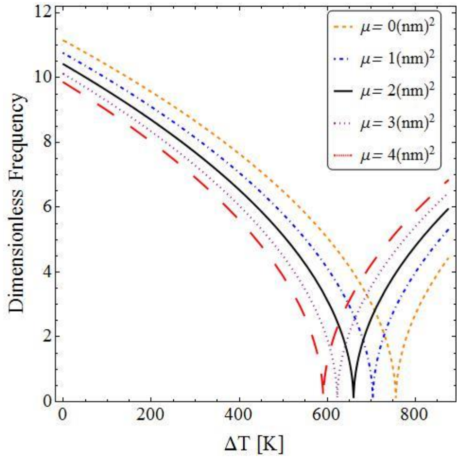

(a) V_E=−0.5 V

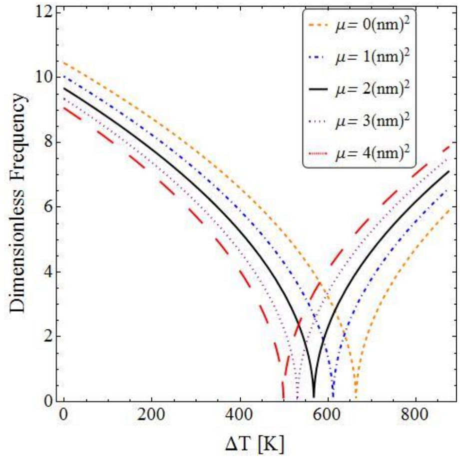

(a) V_E=−0.25 V

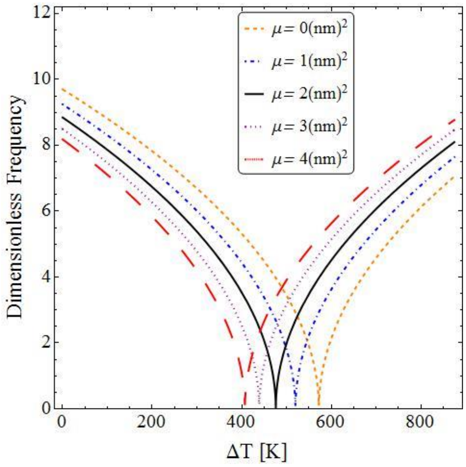

(c) V_E=0 V

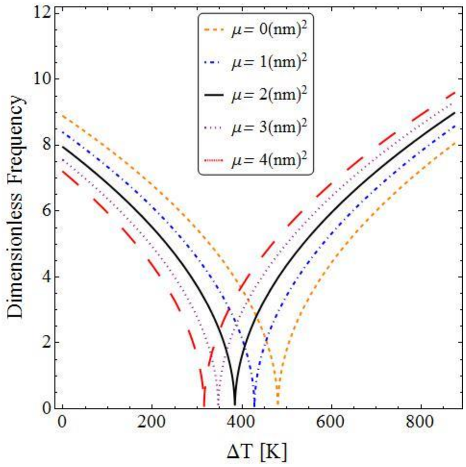

(d) V_E=0.25 V

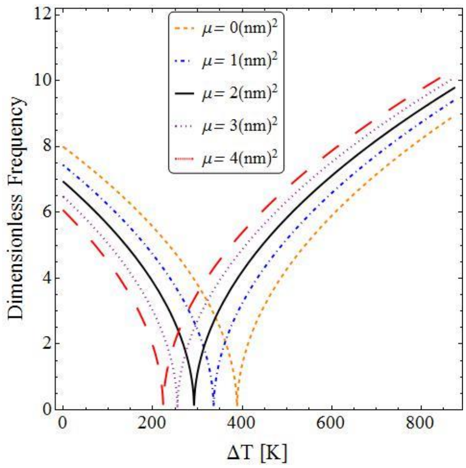

(e) V_E=0.5 V

Fig. 7 Effect of nonlocal parameter on the dimensionless frequency of the S-S FGP nanobeam with respect to non-linear temperature rise for different values of external electric voltage (p=1, L/h=25)

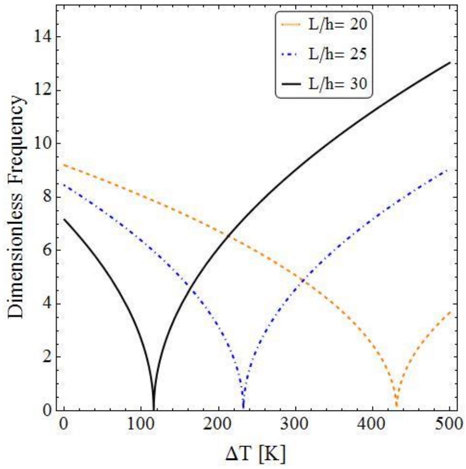

(a) μ=0 (nm)^2

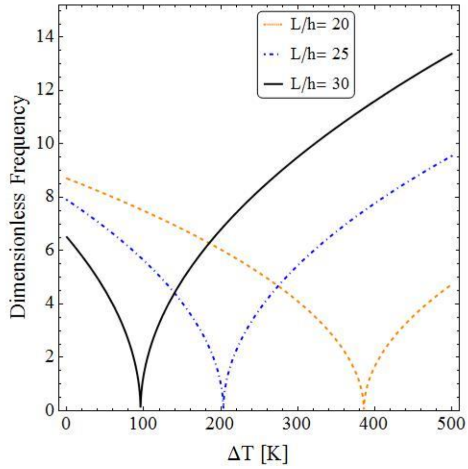

(b) μ=1 (nm)^2

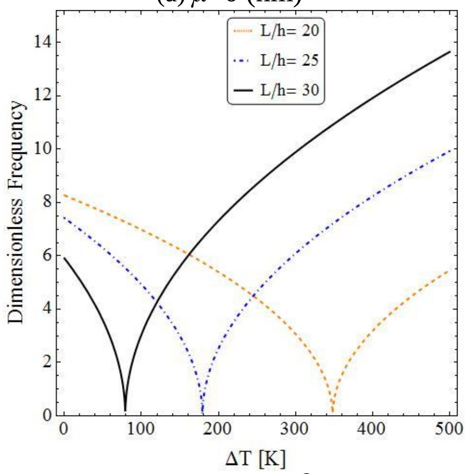

(c) μ=2 (nm)^2

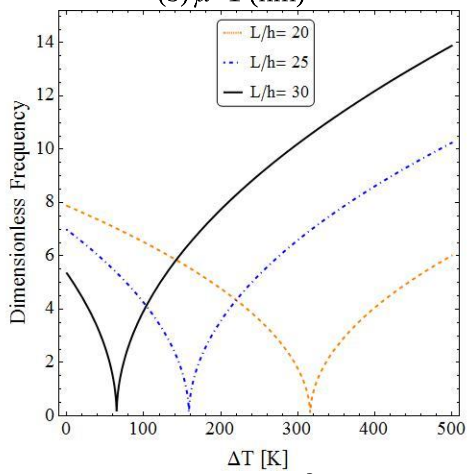

(d) μ=3 (nm)^2

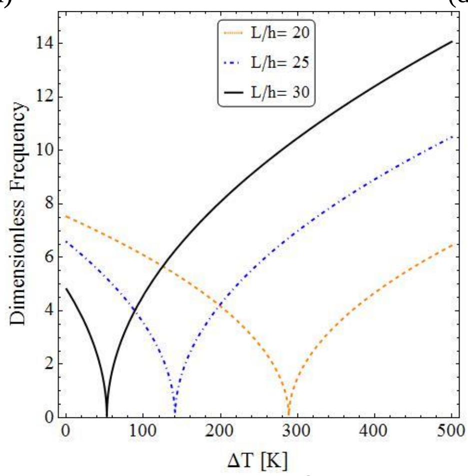

(e) μ=4 (nm)^2

Fig. 8 Effect of aspect ratio on the dimensionless frequency of the S-S FGP nanobeam with respect to uniform temperature rise for different values of nonlocal parameters (p=0.5, V_E=0.5 V)

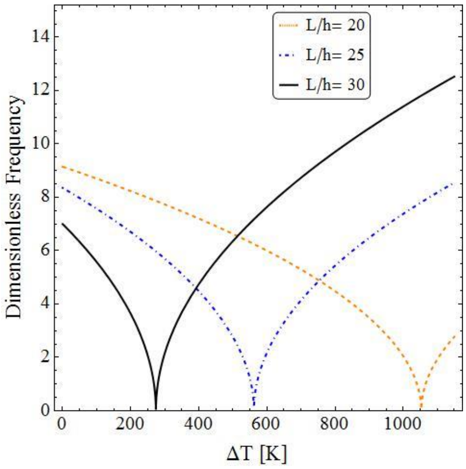

(a) μ=0 (nm)^2

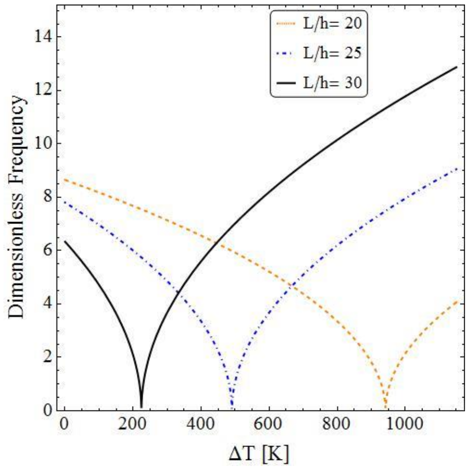

(b) μ=1 (nm)^2

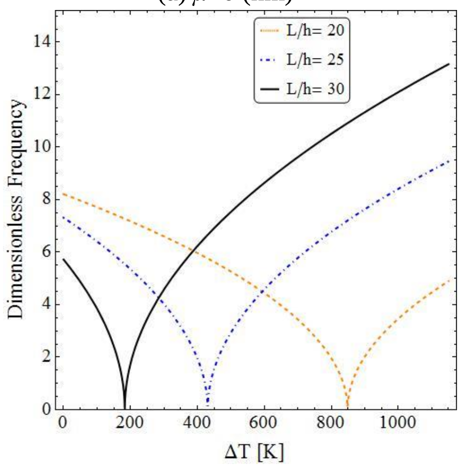

(c) μ=2 (nm)^2

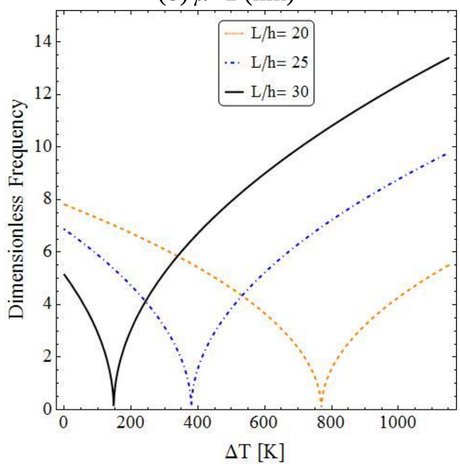

(d) μ=3 (nm)^2

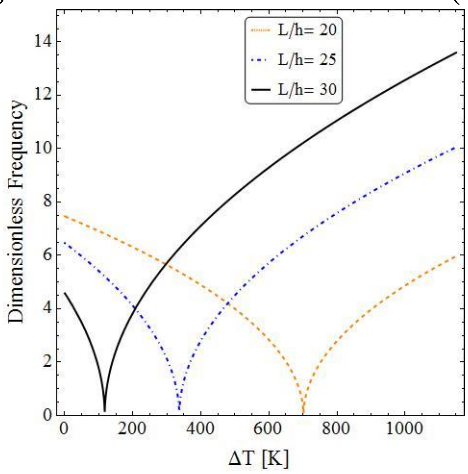

(e) μ=4 (nm)^2

Fig. 9 Effect of aspect ratio on the dimensionless frequency of the S-S FGP nanobeam with respect to linear temperature rise for different values of nonlocal parameters (p=0.5, V_E=0.5 V)

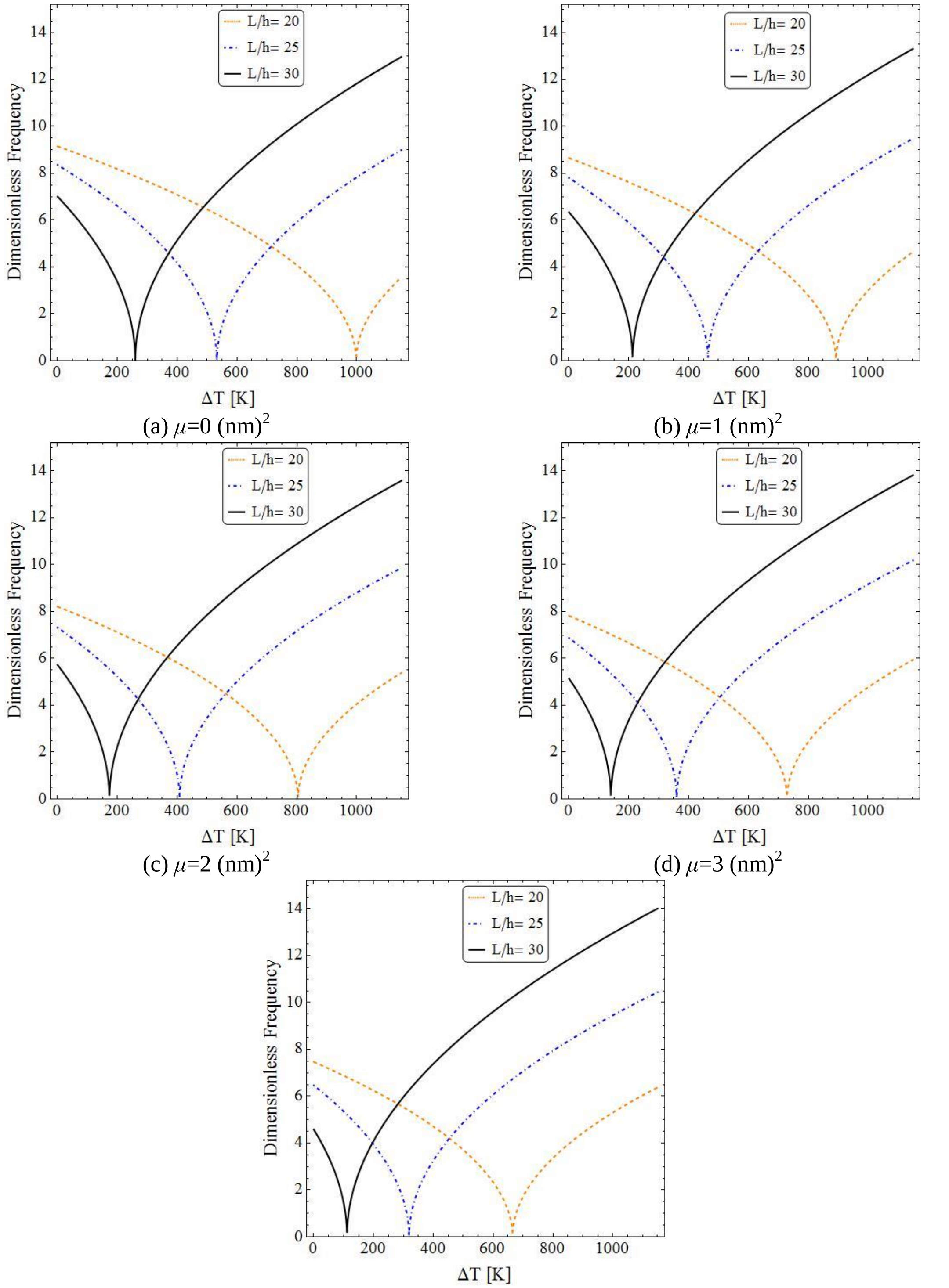

(a) μ=0 (nm)^2 (b) μ=1 (nm)^2

(c) μ=2 (nm)^2 (d) μ=3 (nm)^2

(e) μ=4 (nm)^2

Fig. 10 Effect of aspect ratio on the dimensionless frequency of the S-S FGP nanobeam with respect to non-linear temperature rise for different values of nonlocal parameters (p=0.5, V_E=0.5 V)

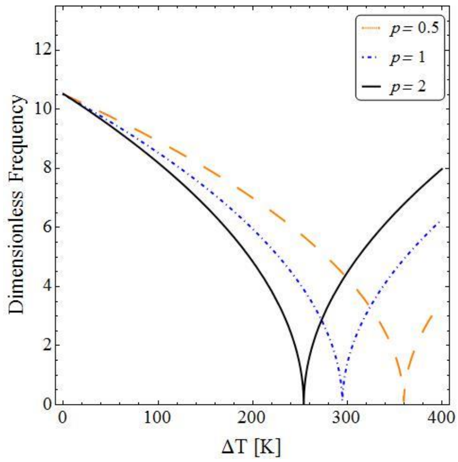

(a) V_E=−0.5 V

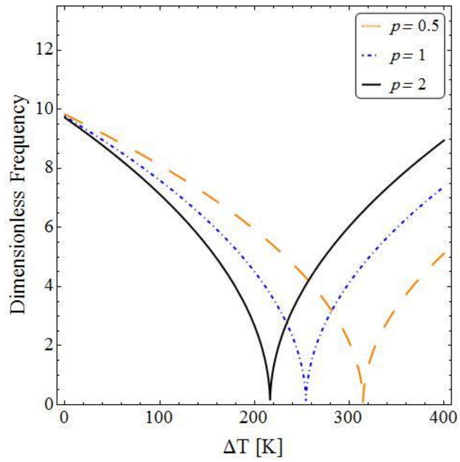

(a) V_E=−0.25 V

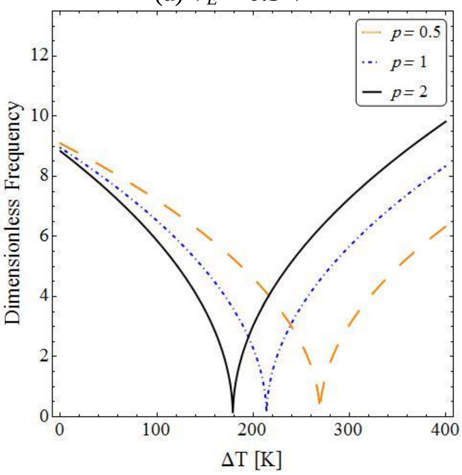

(c) V_E=0 V

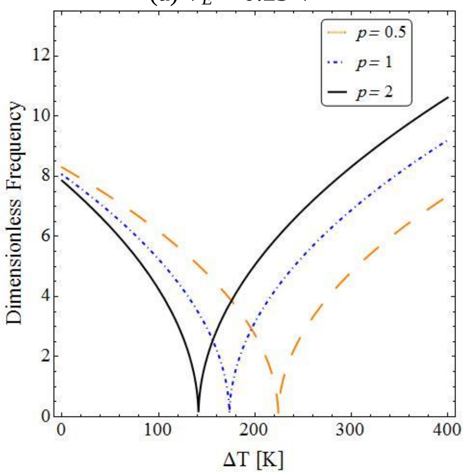

(d) V_E=0.25 V

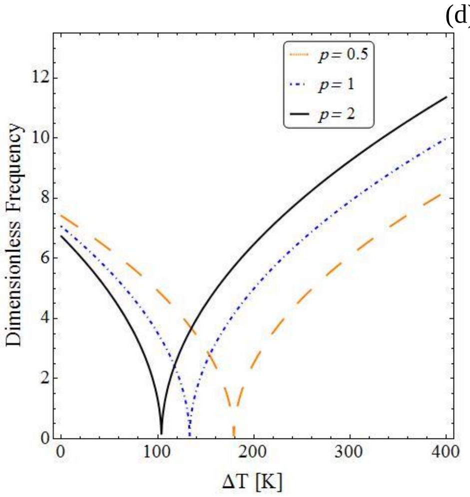

(e) V_E=0.5 V

Fig. 11 Effect of gradient indexes on the dimensionless frequency of the S-S FGP nanobeam with respect to uniform temperature rise for different values of external electric voltage (μ=2 (nm)^2, L/h=25)

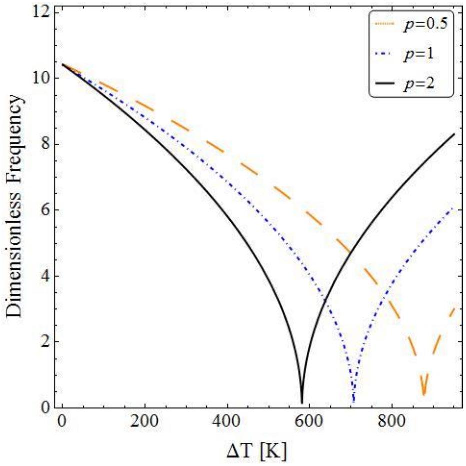

(a) V_E=−0.5 V

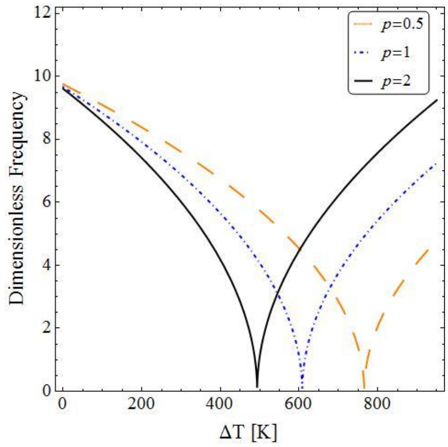

(a) V_E=−0.25 V

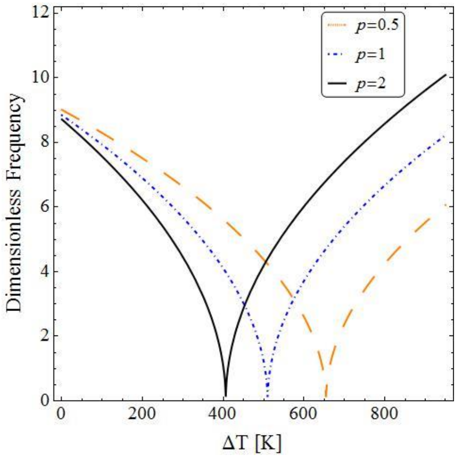

(c) V_E=0 V

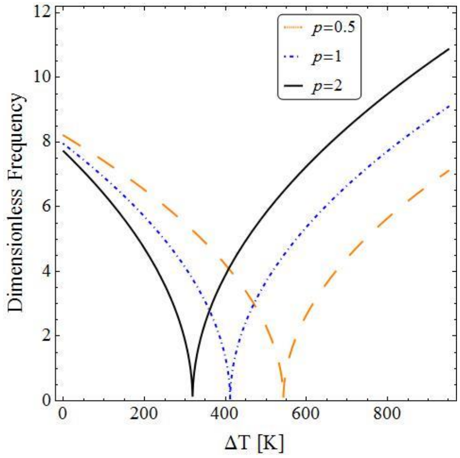

(d) V_E=0.25 V

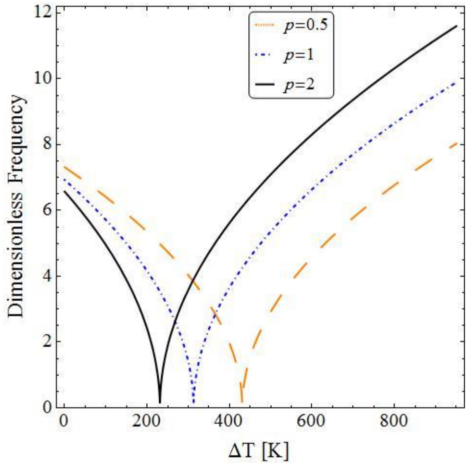

(e) V_E=0.5 V

Fig. 12 Effect of gradient indexes on the dimensionless frequency of the S-S FGP nanobeam with respect to linear temperature rise for different values of external electric voltage (μ=2 (nm)^2, L/h=25)

L/h=25. It is seen that the positive and negative electric voltage respectively decreases and increases the natural frequency. The reason is that compressive and tensile in-plane forces are generated in the graded nanobeams by imposing positive and negative voltages, respectively. In addition, it is observed that the dimensionless frequencies of FGP nanobeam decreases with the increase of temperature until it reaches to zero at the critical temperature point. This is due to the reduction in total stiffness of the beam, since geometrical stiffness decreases when temperature rises. One important observation within the range of temperature before the critical temperature, it is clear that the FGP nanobeams with negative value of applied voltage usually provide larger values of the frequency results. However, this behavior is opposite in the range of temperature beyond the critical temperature. It is also observable that the branching point of the FGP nanobeam is postponed by consideration of the positive external voltage due to the fact that the positive applied voltage parameters result in the decrease of stiffness of the nanostructure. But in order to clarify the effect of the small scale parameter and temperature change on the vibration frequency, Figs. 5-7 intuitively exhibit the variations of the non-dimensional frequency of nonlocal FGP beam with respect to various temperature changes (UTR, LTR and NLTR) for different values of nonlocal parameter and electric voltage at constant slenderness ratio L/h =25 and power-law index p=1. Observing these figures, it is easily deduced for all cases of thermal loading that, an increase in external voltage gives rise to a decrease in the dimensionless natural frequency for all temperature changes. It is clearly observed that the fundamental frequency decreases by increasing temperature changes and it can be stated that temperature change and applied voltage have a notable effect on the fundamental frequency of the graded S-S nanobeam. In addition, the above results obtained also show that the non-dimensional frequencies of the nonlocal FGP model are always smaller than those of the classical graded piezoelectric beam model. With the increase the nonlocal parameter μ from 0 to 4 $(\mathrm{nm})^2$, the natural frequencies decrease significantly. The results indicate that the nonlocal effect is tending to weaken the stiffnes of nanostructures and hence decreases the natural frequencies. Effects of changing length-to-thickness ratio (L/h) on the dimensionless frequency of FGP nanobeam for different values of nonlocality parameter and three types of thermal loading are investigated in Figs. 8-10. In all figures, results are prepared for p=0.5 and V_E=0.5V. It is seen that, small scale parameter, has a softening effect on nonlocal FG beam at pre-buckling region and a rise in small scale increases this effect. Also, regardless of the type of thermal loadings, it can be pointed that the values of natural frequencies decrease with the increasing value of the aspect ratio at a constant material distribution. That is because a higher length-to-thickness ratio indicates that the FGPM nanobeam is thinner with a lower stiffness. Finally, Figs. 11 and 12 display the variations of the first dimensionless natural frequency of the S-S FGP nanobeams with respect to uniform and linear thermal loadings for different values of volume fraction indexes and applied voltage (L/h =25), "The nonlocal parameter is taken to be μ=2$(\mathrm{nm})^2$. The similar conclusions are derived from these figures for the effect of the electric voltage parameter on the natural frequency. It can be concluded from Figs. 11 and 12 that the frequency decreases when the gradient index increases. On the other hand, these figures reveal that the natural frequency magnifies with the decrease of the power-law exponent parameter.

6. Conclusions

This study focuses on the thermo-electro-mechanical free vibration of a size-dependent FGP nanobeam by using Timoshenko beam theory and Eringen's nonlocal elasticity theory. The governing differential equations and related boundary conditions are derived by implementing Hamilton's principle. The Navier solution method is adopted to obtain the analytical solutions of the governing equations of motion. Thermo-electro-mechanical properties of the FGP nanobeams are assumed to be function of thickness and based on power-law model. Accuracy of the results is examined using available data in the literature. Finally, through some parametric study and numerical examples, the effect of different parameters are investigated for graded piezoelectric nanobeams in different set of thermal loading. As shown in several numerical exercises, it is revealed that many parameters such as external electric voltage, small scale parameter, power-law gradient index, various temperature change and aspect ratio have significant impact on non-dimensional frequencies of FGP nanobeams. As previously specified, increasing the nonlocal parameter yields the decrease in dimensionless frequencies for every types of thermal environments. However, the FGP nanobeam model produces smaller natural frequency than the classical beam model. Therefore, the small scale effects should be considered in the analysis of mechanical behavior of nanostructures. The results indicated that the dramatic reduction in frequencies of the nonlocal FGP beam is detected as the increase of the temperature rises and power-law index. Also, it was observed that the effects of external electric voltages on vibration behavior of graded nanobeam are dependent on their sign.

References

Bodaghi, M., Damanpack, A.R., Aghdam, M.M. and Shakeri, M. (2014), "Geometrically non-linear transient thermo-elastic response of FG beams integrated with a pair of FG piezoelectric sensors", *Compos. Struct.*, **107,** 48-59.

Carbonari, R.C., Silva, E.C. and Paulino, G.H. (2009), "Multi-actuated functionally graded piezoelectric micro-tools design: A multiphysics topology optimization approach", *Int. J. Numer. Meth. Eng.*, **77**(3), 301-336.

Doroushi, A., Eslami, M.R. and Komeili, A. (2011), "Vibration analysis and transient response of an FGPM beam under thermo-electro-mechanical loads using higher-order shear deformation theory", *J. Intel. Mater. Syst. Struct.*, **22**(3), 231-243.

Ebrahimi, F. and Barati, M.R. (2015), "A nonlocal higher-order shear deformation beam theory for vibration analysis of size-dependent functionally graded nanobeams", *Arab. J. Sci. Eng.*, 1-12.

Ebrahimi, F. and Erfan, S. (2015e), "A semi-analytical method for vibrational and buckling analysis of functionally graded nanobeams considering the physical neutral axis position", *CMES: Comput. Model. Eng. Sci.*, **105**, 151-181

Ebrahimi, F. and Rastgo, A. (2008), "An analytical study on the free vibration of smart circular thin FGM plate based on classical plate theory", *Thin Wall. Struct.*, **46**(12), 1402-1408.

Ebrahimi, F. and Salari, E. (2015a), "Effect of various thermal loadings on buckling and vibrational characteristics of nonlocal temperature-dependent FG nanobeams", *Mech. Adv. Mater. Struct.,* **23**(12), 1379-1397.

Ebrahimi, F. and Salari, E. (2015b), "Thermo-mechanical vibration analysis of nonlocal temperature-dependent FG nanobeams with various boundary conditions", *Compos. Part B: Eng.*, **78**, 272-290.

Ebrahimi, F. and Salari, E. (2015c), "Thermal buckling and free vibration analysis of size dependent Timoshenko FG nanobeams in thermal environments", *Compos. Struct.*, **128**, 363-380.

Ebrahimi, F. and Salari, E. (2015d), "Size-dependent free flexural vibrational behavior of functionally graded nanobeams using semi-analytical differential transform method", *Compos. Part B: Eng.*, **79**, 156-169.

Ebrahimi, F. and Zia, M. (2015), "Large amplitude nonlinear vibration analysis of functionally graded

Timoshenko beams with porosities", *Acta Astronautica*, **116**, 117-125.

Ebrahimi, F., Ghadiri, M., Salari, E., Hoseini, S.A.H. and Shaghaghi, G.R. (2015b), "Application of the differential transformation method for nonlocal vibration analysis of functionally graded nanobeams", *J. Mech. Sci. Tech.*, **29**(3), 1207-1215.

Ebrahimi, F., Rastgoo, A. and Atai, A.A. (2009), "A theoretical analysis of smart moderately thick shear deformable annular functionally graded plate", *Euro. J. Mech. A/Solid.*, **28**(5), 962-973.

Ebrahimi, F., Salari, E. and Hosseini, S.A.H. (2015a), "Thermomechanical vibration behavior of FG nanobeams subjected to linear and non-linear temperature distributions", *J. Therm. Stress.*, **38**(12), 1362-1388.

Eltaher, M.A., Emam, S.A. and Mahmoud, F.F. (2012), "Free vibration analysis of functionally graded size-dependent nanobeams", *Appl. Math. Comput.*, **218**(14), 7406-7420.

Eringen, A.C. (1983), "On differential equations of nonlocal elasticity and solutions of screw dislocation and surface waves", *J. Appl. Phys.*, **54**(9), 4703-4710.

Eringen, A.C. (2002), *Nonlocal continuum field theories*, Springer Science & Business Media.

Fei, P., Yeh, P.H., Zhou, J., Xu, S., Gao, Y., Song, J. and Wang, Z.L. (2009), "Piezoelectric potential gated field-effect transistor based on a free-standing ZnO wire", *Nano Lett.*, **9**(10), 3435-3439.

Fu, Y., Du, H. and Zhang, S. (2003), "Functionally graded TiN/TiNi shape memory alloy films", *Mater. Lett.*, **57(**20), 2995-2999.

He, J.H., Hsin, C.L., Liu, J., Chen, L.J. and Wang, Z.L. (2007), "Piezoelectric gated diode of a single ZnO nanowire", *Adv. Mater.*, **19**(6), 781-784.

Hosseini-Hashemi, S. and Nazemnezhad, R. (2013), "An analytical study on the nonlinear free vibration of functionally graded nanobeams incorporating surface effects", *Compos. Part B: Eng.*, **52**, 199-206.

Iijima, S. (1991), "Helical microtubules of graphitic carbon", *Nature*, **354**, 56-58.

Ke, L.L. and Wang, Y.S. (2012), "Thermoelectric-mechanical vibration of piezoelectric nanobeams based on the nonlocal theory", *Smart Mater. Struct.*, **21**(2), 025018.

Ke, L.L., Wang, Y.S. and Wang, Z.D. (2012a), "Nonlinear vibration of the piezoelectric nanobeams based on the nonlocal theory", *Compos. Struct.*, **94**(6), 2038-2047.

Ke, L.L., Wang, Y.S., Yang, J. and Kitipornchai, S. (2012b), "Nonlinear free vibration of size-dependent functionally graded microbeams", *Int. J. Eng. Sci.*, **50**(1), 256-267.

Kerman, K., Lai, B.K. and Ramanathan, S. (2012), "Nanoscale compositionally graded thin-film electrolyte membranes for low-temperature solid oxide fuel cells", *Adv. Energy Mater.*, **2**(6), 656-661.

Kiani, Y. and Eslami, M.R. (2013), "An exact solution for thermal buckling of annular FGM plates on an elastic medium", *Compos. Part B: Eng.*, **45**(1), 101-110.

Kim, H.S., Yang, Y., Koh, J.T., Lee, K.K., Lee, D.J., Lee, K.M. and Park, S.W. (2009), "Fabrication and characterization of functionally graded nano-micro porous titanium surface by anodizing", *J. Biomed. Mater. Res. Part B: Appl. Biomater.*, **88**(2), 427-435.

Komijani, M., Kiani, Y., Esfahani, S.E. and Eslami, M.R. (2013), "Vibration of thermo-electrically post-buckled rectangular functionally graded piezoelectric beams", *Compos. Struct.*, **98**, 143-152.

Komijani, M., Reddy, J.N. and Eslami, M.R. (2014), "Nonlinear analysis of microstructure-dependent functionally graded piezoelectric material actuators", *J. Mech. Phys. Solid.*, **63**, 214-227.

Lee, Z., Ophus, C., Fischer, L.M., Nelson-Fitzpatrick, N., Westra, K.L., Evoy, S., Radmilovic, V., Dahmen, U. and Mitlin, D. (2006), "Metallic NEMS components fabricated from nanocomposite Al-Mo films", *Nanotechnol.*, **17**(12), 3063.

Lezgy-Nazargah, M. (2015), "Fully coupled thermo-mechanical analysis of bi-directional FGM beams using NURBS isogeometric finite element approach", *Aerosp. Sci. Tech.*, **45**, 154-164.

Lezgy-Nazargah, M., Vidal, P. and Polit, O. (2013), "An efficient finite element model for static and dynamic analyses of functionally graded piezoelectric beams", *Compos. Struct.*, **104**, 71-84.

Lü, C.F., Lim, C.W. and Chen, W.Q. (2009), "Size-dependent elastic behavior of FGM ultra-thin films based on generalized refined theory", *Int. J. Solid. Struct.*, **46**(5), 1176-1185.

Lun, F.Y., Zhang, P., Gao, F.B. and Jia, H.G. (2006), "Design and fabrication of micro optomechanical vibration sensor", *Microfabric. Tech.*, **120**(1), 61-64.

Nateghi, A. and Salamat-talab, M. (2013), "Thermal effect on size dependent behavior of functionally graded microbeams based on modified couple stress theory", *Compos. Struct.*, **96**, 97-110.

Niknam, H., and Aghdam, M.M. (2015), "A semi analytical approach for large amplitude free vibration and buckling of nonlocal FG beams resting on elastic foundation", *Compos. Struct.*, **119**, 452-462.

Pradhan, S.C. and Mandal, U. (2013), "Finite element analysis of CNTs based on nonlocal elasticity and Timoshenko beam theory including thermal effect", *Physica E: Low-dimens. Syst. Nanostruct.*, **53**, 223-232.

Rahaeifard, M., Kahrobaiyan, M.H. and Ahmadian, M.T. (2009), "Sensitivity analysis of atomic force microscope cantilever made of functionally graded materials", *International Design Engineering Technical Conferences and Computers and Information in Engineering Conference*, American Society of Mechanical Engineers.

Rahmani, O. and Pedram, O. (2014), "Analysis and modeling the size effect on vibration of functionally graded nanobeams based on nonlocal Timoshenko beam theory", *Int. J. Eng. Sci.*, **77**, 55-70.

Shi, Z.F. and Chen, Y. (2004), "Functionally graded piezoelectric cantilever beam under load", *Arch. Appl. Mech.*, **74**(3-4), 237-247.

Tanner, S.M., Gray, J.M., Rogers, C.T., Bertness, K.A. and Sanford, N.A. (2007), "High-Q GaN nanowire resonators and oscillators", *Appl. Phys. Lett.*, **91**(20), 203117.

Wan, Q., Li, Q.H., Chen, Y.J., Wang, T.H., He, X.L., Li, J.P. and Lin, C.L. (2004), "Fabrication and ethanol sensing characteristics of ZnO nanowire gas sensors", *Appl. Phys. Lett.*, **84**(18), 3654-3656.

Wang, Q. (2002), "On buckling of column structures with a pair of piezoelectric layers", *Eng. Struct.*, **24**(2), 199-205.

Wang, Z.L. and Song, J. (2006), "Piezoelectric nanogenerators based on zinc oxide nanowire arrays", *Science*, **312**(5771), 242-246.

Witvrouw, A. and Mehta, A. (2005), "The use of functionally graded poly-SiGe layers for MEMS applications", *Mater. Sci. Forum*, **492**, 255-260.

Xiang, H.J. and Shi, Z.F. (2009), "Static analysis for functionally graded piezoelectric actuators or sensors under a combined electro-thermal load", *Euro. J. Mech. A/Solid.*, **28**(2), 338-346.

Yang, J. and Xiang, H.J. (2007), "Thermo-electro-mechanical characteristics of functionally graded piezoelectric actuators", *Smart Mater. Struct.*, **16**(3), 784.

Zhang, D.G. (2013), "Nonlinear bending analysis of FGM beams based on physical neutral surface and high order shear deformation theory", *Compos. Struct.*, **100**, 121-126.

Zhong, Z. and Yu, T. (2007), "Electroelastic analysis of functionally graded piezoelectric material beams", *J. Intel. Mater. Syst. Struct.*, doi: 10.1177/1045389X07079453.

Zhu, X. and Meng, Z. (1995), "Operational principle, fabrication and displacement characteristics of a functionally gradient piezoelectric ceramic actuator", *Sens. Actuat. A: Phys.*, **48**(3), 169-176.

JL